NUMERICAL STUDY OF RADIATION ON NATURAL CONVECTION FLOW ON A SPHERE WITH HEAT GENERATION

by

MD. MIRAJ ALI
Student No. 040409001F
Registration No. 0404391, Session: April-2004

MASTER OF PHILOSOPHY
IN
MATHEMATICS

Department of Mathematics
BANGLADESH UNIVERSITY OF ENGINEERING AND TECHNOLOGY, DHAKA-1000
January- 2007

The thesis titled

NUMERICAL STUDY OF RADIATION ON NATURAL CONVECTION FLOW ON A SPHERE WITH HEAT GENERATION

Submitted by

MD. MIRAJ ALI

Student No. 040409001F, Registration No. 0404391, Session: April-2004, a full time student of M. Phil. (Mathematics) has been accepted as satisfactory in partial fulfillment for the degree of

Master of Philosophy in Mathematics

on 15, January- 2007

BOARD OF EXAMINERS

1. A. Alim
   Dr. Md. Abdul Alim — Chairman (Supervisor)
   Assistant Professor
   Dept. of Mathematics, BUET, Dhaka-1000

2. _____
   Dr. Md. Arif Hasan Mamun — Member (Co-Supervisor)
   Assistant Professor
   Dept. of Mechanical Engineering
   BUET, Dhaka-1000

3. _____
   Dr. Md. Abdul Maleque — Member
   Associate Professor
   Dept. of Mathematics, BUET, Dhaka-1000

4. _____
   Dr. Md. Mustafa Kamal Chowdhury — Member (Ex-Officio)
   Professor and Head
   Dept. of Mathematics, BUET, Dhaka-1000

5. _____
   Dr. Md. Mashud Karim — Member (External)
   Associate Professor
   Dept. of Naval Architecture and Marin Engineering
   BUET, Dhaka-1000

Abstract

In this thesis, the effects of radiation on natural convection flow on a sphere in presence of heat generation and the effects of radiation on magnetohydrodynamic (MHD) natural convection flow on a sphere in presence of heat generation have been investigated. The physical problems are represented mathematically by different sets of governing equations along with the corresponding boundary conditions. Using the appropriate transformation, the governing equations containing the equations of continuity, momentum and energy are transformed into a set of non-dimensional boundary layer equations along with the corresponding boundary conditions, which are then solved numerically using finite-difference method together with the Keller box scheme. Here, the attention is focused on the evaluation of the surface shear stress in terms of local skin friction, rate of heat transfer in terms of local Nusselt number, velocity profiles as well as temperature profiles. The software FORTRAN 90 is used to perform computational job and the post processing software TECHPLOT has been used to display the numerical results graphically. A selection of parameters set is also considered for computation consisting of heat generation parameter Q, radiation parameter Rd, surface temperature parameter θ_w, Prandtl number Pr and magnetic parameter M. The results in terms of local skin friction, local Nusselt number will be shown in tabular forms. Velocity profiles, temperature profiles, skin friction coefficient and rate of heat transfer have been displayed graphically for various values of heat generation parameter, radiation parameter and surface temperature parameter separately and the Prandtl number as well.

Author's Declaration

I am hereby declaring that the work in this dissertation was being carried out in accordance with the regulations of Bangladesh University of Engineering and Technology (BUET), Dhaka, Bangladesh .The work is also original except where indicated by and attached with special reference in the context and no part of it has been submitted for any attempt to get other degrees or diplomas.

All views expressed in the dissertation are those of the author and in no way or by no means represent those of Bangladesh University of Engineering and Technology, Dhaka. This dissertation has not been submitted to any other University for examination either in home or abroad.

(Md. Miraj Ali)

Date: 15 January 2007

Acknowledgements

To my great delight, I would like to have the opportunity to express my heart-rendering appreciation and profound sense of gratitude to my Supervisor Dr. Md. Abdul Alim, Assistant Professor, Department of Mathematics and Co-supervisor Dr. Md. Arif Hasan Mamun, Assistant Professor, Department of Mechanical Engineering, BUET who have encouraged and rightly initiated me to step into the wide arena of mathematics and its application in the engineering fields.

I am not less grateful and thankful to the efforts, perseverance, sincerity, enormous will-force, clarity, accuracy, completeness, monumental patience, generous co-operation and fellow-feeling they made for me to venture this research and bring this painstaking task to a successful end.

I am also deeply indebted to Prof. Dr. Nilufar Farhat Hossain , the formerly Head of the Department of Mathematics and Prof. Dr. Md. Mustafa Kamal Chowdhury, the present Head of the Department of Mathematics, BUET for their wise and liberal co-operation in providing me all necessary help from the department during my course of M.Phil.degree.

I would also like to extend my thanks to all other teachers and concerned of this department for their thoroughly help and co-operation. It is also a subject of joy for me to thank Prof. Kazi Md. Nurul Islam Faruky, Principal of Dhaka Commerce College for his visionary encouragement to complete the M.Phil degree.

It is with particular pleasure to express my gratefulness to Md. Mustafizur Rahman, Assistant Professor, Department of Mathematics, BUET, and Md. Mahmud Alam, Assistant Professor, Department of Mathematics, DUET, Gazipur, for their inspiration and unhindered co-operation to bring this venture to a meaningful conclusion. Finally, I must acknowledge my debt to my parents for whom I have been able to see the beautiful sights and sounds of the world. Last but not the least, it would be ungrateful for me if I do not evaluate the efforts and pains my wife taken during the struggle-some course.

Contents

Nomenclature

a	Radius of the sphere
a_r	Rosseland mean absorption co-efficient
C_f	Local skin friction coefficient
C_p	Specific heat at constant pressure
f	Dimensionless stream function
f'	Derivative of f with respect to y
Gr	Grashof number
g	Acceleration due to gravity
k	Thermal conductivity
M	Magnetic parameter
Nu	Local Nusselt number
Pr	Prandtl number
Q	Heat generation parameter
q_r	Radiation heat flux
q_w	Heat flux at the surface
q_c	Conduction heat flux.
Rd	Radiation parameter
r	Radial distance from the symmetric axis to the surface
T	Temperature of the fluid in the boundary layer
T_∞	Temperature of the ambient fluid
T_w	Temperature at the surface
$(\hat{u},\hat{v})$	Dimensionless velocity components along the $(\hat{x},\hat{y})$ axes
(u,v)	Dimensionless velocity components along the (x,y) axes
x, y	Axis in the direction along and normal to the surface respectively

Greek symbols

β	Coefficient of thermal expansion
β_0	Strength of magnetic field
θ	Dimensionless temperature function
θ_w	Surface temperature parameter
μ	Viscosity of the fluid
ν	Kinematic viscosity
ρ	Density of the fluid
σ	Stephman-Boltzman constant.
σ_s	Scattering co-efficient
σ_0	Electrical conduction
τ_w	Shearing stress
ψ	Non-dimensional stream function

List of Tables

List of Figures

Chapter 1

1.1 Introduction

The effects of radiation on free convection boundary layer over or on various shapes such as vertical flat plate, cylinder, sphere etc, have been studied by many investigators and it has been a very popular research topic for many years. It is readily recognized that a wealth of information is now available on convective heat and mass transfer for viscous (Newtonian) fluids. Radiation effects on free convection flow are important in the context of space technology and processes involving high temperatures but comparatively less information about the effects of radiation on the boundary layer flow is available than convection and conduction heat transfer from fluid past a body.

A study of the flow of electrically conducting fluid in presence of magnetic field is also important from the technical point of view and such types of problems have received much attention by many researchers. The specific problem selected for study is the flow and heat transfer in an electrically conducting fluid adjacent to the surface. The interaction of the magnetic field and the moving electric charge carried by the flowing fluid induces a force which tends to oppose the fluid motion. And near the leading edge, the velocity is very small so that the magnetic force which is proportional to the magnitude of the longitudinal velocity and acts in the opposite direction is also very small. Consequently, the influence of the magnetic field on the boundary layer is exerted only through induced forces within the boundary layer itself without additional effects arising from the free stream pressure gradient. Solid matter is generally excluded from magnetohydrodynamics effect, but it should be realized that the same principles will apply. Electrical conduction in metals and the Hall effect are two examples.

The study of temperature and heat transfer is of great importance to the engineers because of its almost universal occurrence in many branches of science and engineering. Although heat transfer analysis is most important for the proper sizing of fuel elements in the nuclear reactors cores to prevent burnout. The performance of aircraft also depends upon the ease with which the structure and engines can be cooled. The design of chemical plants is usually

done on the basis of heat transfer analysis and the analogous mass transfer processes. The amount of energy transfer as heat can be determined from energy-conservation consideration (first law of thermodynamics). Energy transfer as heat will take place from the assembly (body) with the higher temperature, if these two are permitted to interact through a diathermal wall (second law of thermodynamics). The transfer and conversion of energy from one form to another is the basis to all heat transfer process and hence, they are governed by the first as well as the second law of thermodynamics. Heat transfer is commonly associated with fluid dynamics. The knowledge of temperature distribution is essential in heat transfer studies because of the fact that the heat flow takes place only wherever there is a temperature gradient in a system. The heat flux which is defined as the amount of heat transfer per unit area in per unit time can be calculated from the physical laws relating to the temperature gradient and the heat flux.

When a body is introduced into a fluid at different temperatures forms a source of equilibrium disturbance due to the thermal interaction between the body and the fluid. The fluid elements near the body surface assume the temperature of the body and then begin the propagation of heat into the fluid and the variation of temperature is accompanied by density variations. In particular, if the density variation is caused by the non-uniformity of the temperature is called convection. The convective mode of heat transfer is generally divided into two basic processes. If the motion of the fluid arises from an external agent then the process is termed forced convection. This type of fluid flow is caused in general by a fan, blower, the bursting of a tyre etc. Such problems are very frequently encountered in technology where the heat transfers to or from a body is often due to imposed flow of a fluid of different temperature from that of the body. On the other hand, if no such externally induced flow is provided and the flow arises from the effect of a density difference resulting from temperature or concentration difference, in a body forced field such as the gravitational field, then the process is termed natural convection. Generally, the density difference gives rise to buoyancy forces, which drive the flow. Buoyancy induced convective flow is of great importance in many heat removal processes in engineering technology and has attracted the attention of many researchers in the last few decades due to the fact that both science and technology are being interested in passive energy storage systems, such as the cooling of spent fuel rods in nuclear power applications and the design of solar collectors. In particular,

it has been ascertained that free convection induced the thermal stress, which leads to critical structural damage in the piping systems of nuclear reactors. The buoyant flow arising from heat rejection to the atmosphere, heating of rooms, fires, and many other heat transfers processes, both natural and artificial, are other examples of natural convection flows. Nazar et al. (2002a, 2002b) considered the free convection boundary layer flow on an isothermal horizontal circular cylinder and on an isothermal sphere. Yao (1983) has studied the problem of natural convection flow along a vertical wavy surface. Also the problem of free convection boundary layer on a vertical plate with prescribed surface heat flux investigated by Merkin and Mahmood (1990).

The governing partial differential equations are to deal with in the case of incompressible viscous fluid such as continuity equation, momentum equation and energy equation. The radiation energy emitted by a body is transmitted in the space in the form of electromagnetic waves according to Maxwell's classic electromagnetic wave theory or in the form of discrete photons according to Planck's hypothesis. Both concepts have been utilized in the investigation of radiative-heat transfer. The emission or absorption of radiation energy by a body is a bulk process; that is, radiation originating from the interior of the body is emitted through the surface. Conversely, radiation incident on the surface of a body penetrates to the depths of the medium where it is attenuated. When a large proportion of the incident radiation is attenuated within a very short distance from the surface, we may speak of radiation as being absorbed or emitted by the surface. For example, thermal radiation incident on a metal surface is attenuated within a distance of a few angstroms, from the surface; hence metals are opaque to thermal radiation.

Magnetohydrodynamic (MHD) is the science, which deals with the motion of a highly conducting fluid in presence of a magnetic field. The motion of the conducting fluid across the magnetic field generates electric currents which change the magnetic field and the action of the magnetic field on these currents give rise to mechanical forces, which modify the fluid. It is possible to attain equilibrium in a conducting fluid if the current is parallel to the magnetic field. For then, the magnetic forces vanish and the equilibrium of the gas is the same as in the absence of magnetic fields are considered force free. But most liquids and gases are poor conductors of electricity. In the case when the conductor is either a liquid or a gas, electromagnetic forces will be generated which may be of the same order of magnitude

as the hydrodynamical and inertial forces. Thus the equations of motion as well as the other forces will have to take these electromagnetic forces into account. The MHD was originally applied to astrophysical and geophysical problems, where it is still very important but more recently to the problem of fusion power where the application is the creation and containment of hot plasmas by electromagnetic forces, since material walls would be destroyed. Astrophysical problems include solar structure, especially in the outer layers, the solar wind bathing the earth and other planets, and interstellar magnetic fields. The primary geophysical problem is planetary magnetism, produced by currents deep in the planet, a problem that has not been solved to any degree of satisfaction. MHD free convection flow of visco-elastic fluid past an infinite porous plate was investigated by Chowdhury and Islam (2000).Raptis and Kafousian (1982) have investigated the problem of magnetohydrodynamic free couvection flow and mass transfer through a porous medium bounded by an infinite vertical porous plate with constant heat flux. Moreover, Hossian and Ahmed (1990) and Hossian et al. (1997), discussed the both forced and free convection boundary layer flow of an electrically conducting fluid in presence of magnetic field.

However, it is possible to make some gases very highly conducting by ionizing them. For ionization to take effect, the gas must be very hot at temperature upwards of 5000^{0} k or so. Such ionized gases are called plasmas. The material within a star of plasma is of very high conductivity and it exists within a strong magnetic field.

The study of heat generatiou or absorption in moving fluids is important in problems dealing with chemical reactions and those concerned with dissociating fluids. Possible heat generation effects may alter the temperature distribution; consequently, the particle deposition rate in nuclear reactors, electronic chips and semiconductor waters. In fact, the literature is replete with examples dealing with the heat transfer in laminar flow of viscous fluids. Vajravelu and Hadjinolaou (1993) studied the heat transfer characteristics in the laminar boundary layer of a viscous fluid over a stretching sheet with viscous dissipation or frictional heating and internal heat generation.

Many mathematicians, versed engineers and researchers have studied the Problems of free convection boundary layer flow over or on a various types of shapes. Amongst them are Hossain et al (1996), Huang and Chen (1987), Merkin and Mahmood (1990), Nazar et al

(2002a, 2002b) and Molla et al (2004). Huang and Chen (1987), Nazar et al (2002a, 2002b) consider the free convection boundary layer an isothermal sphere and on an isothermal horizontal circular cylinder both in a micropolar fluid. Molla et al (2004) have studied the problem of natural convection flow along a vertical wavy surface with uniform surface temperature in presence of heat generation or absorption. The problem of the free convection boundary layer on a vertical plate with prescribed surface heat flux was studied by Merkin and Mahmood (1990). Also the effects of axial heat conduction in a vertical plate on free convection heat transfer have studied by Miyamoto et al. (1980). On the other hand, the coupling of conduction with laminar natural convection boundary layer flow along a flat plate was investigated by Pozzi and Lupo (1988).

A transformation of the boundary layer equations for natural convection flow past a vertical plate with an arbitrary blowing and wall temperature variations was studied by Vedhanayagam et al. (1980). The case of a heated isothermal horizontal surface with transpiration was discussed in some detail first by Clarke and Riley ((1975, 1976), and then recently by Lin and Yu (1988). Hossain and Takhar (1996) also discussed the same things but with the temperature dependent viscosity and thermal conductivity. Soundalgekar et al. (1960) have studied radiation effects on free convection flow of a gas past a semi-infinite flat plate using the Cogley-Vincenti-Giles equilibrium model Cogley et al(1968), later Hossain and Takhar (1996) have analyzed the effects of radiation using the Rosseland diffusion approximation which leads to non-similar solutions for free convection flow past a heated vertical plate. Limitations of this approximation are discussed briefly in Özisik (1973).

A study of the flow of electrically conducting fluid in presence of magnetic field is also important from the technical point of view and such types of problems have received much attention by many researchers. Kuiken (1970) have studied the problem of magnetohydrodynamic free convection in a strong cross field and also the effect of magnetic field on free convection heat transfer have studied by Sparrow and Cess (1961). Elbashbeshy (2000) also discussed the effect of free convection flow with variable viscosity and thermal diffusivity along a vertical plate in the presence of magnetic field. But Hossain (1992) introduced the viscous and joule heating effects on MHD free convection flow with variable plate temperature. Also Hossain et al. (1998) have investigated the heat transfer response of MHD free convection flow along a vertical plate to surface temperature oscillation. Very

recently Ahmad and Zaidi (2004) investigated the magnetic effect on over back convection through vertical stratum. Hossain et al. (1997) discussed the free convection boundary layer flow of an electrically conducting fluid in presence of magnetic field. Taher et al. (2004) studied magnetohydrodynamic natural convection flow on a sphere. The effect of conjugate natural convection flow on or from various heated shapes has been studied by Merkin and Pop (1982), Vynnycky and Kimura (1982), Kimura et al (1998) and Yu and Lin (1982). Also the problem of the conjugate conduction natural convection heat transfer along a thin vertical plate with non uniform heat generation have studied by Mendez and Trevino (2000). Cheng (1982) studied the mixed convection along a horizontal cylinder and along a sphere in a saturated porous medium. Taher and Molla (2005) studied natural convection boundary layer flow on a sphere in presence of heat generation and then Molla et al. (2005) have studied magnetohydrodynamic natural convection flow on a sphere in presence of heat generation.

In the present work, the effects of radiation on free convection flow around a sphere in presence of heat generation have been investigated. The results were obtained for different values of relevant physical parameters. The natural convection boundary layer flow on a sphere of an electrically conducting and steady viscous incompressible fluid in presence of strong magnetic field and heat generation with constant heat flux has been considered.

The governing partial differential equations are reduced to locally non-similar partial differential forms by adopting appropriate transformations. The transformed boundary layer equations are solved numerically using implicit finite difference method together with Keller box scheme by Keller (1978) and later by Cebeci and Bradshaw (1984). Here, the attention is focused on the evolution of the surface shear stress in terms of local skin friction and the rate of heat transfer in terms of local Nusselt number, velocity profiles as well as temperature profiles for selected values of parameters consisting of heat generation parameter Q, the magnetic parameter M, Prandtl number Pr and the radiation parameter Rd.

In chapter 2, the effects of radiation on natural convection flow on a sphere have been investigated in presence of heat generation. The non-dimensional boundary layer equations are solved by using implicit finite difference methods by Keller (1978), Cebeci and Bradshaw (1984). The results in terms of local skin friction, local Nusselt number will be shown in tabular forms. Velocity profiles, temperature profiles, skin friction coefficient and

the rate of heat transfer have been displayed graphically for various values of heat generation parameter, radiation parameter and surface temperature parameter separately and the Prandtl number as well. Some results for skin friction coefficient and the rate of heat transfer for different values heat generation parameter have presented in tabular form.

In chapter-3, the effects of radiation on magnetohydrodynamic natural convection flow on a sphere have been investigated in presence of heat generation. Numerical results have been shown in terms of local skin friction, rate of heat transfer, velocity profiles as well as temperature profiles for a selection of relevant physical parameters set are shown graphically. Some results for skin friction coefficient and the rate of heat transfer for different values magnetic parameter have presented in tabular form as well. Present numerical results have been compared with the results of Nazar et al. (2002) and Huang and Chen (1987).

Chapter 2

Effect of Radiation on Natural Convection Flow on a Sphere in Presence of Heat Generation

2.1 Introduction

This chapter describes the effect of radiation on natural convection flow on a sphere in presence of heat generation. The natural convection laminar flow from an isothermal sphere immersed in a viscous incompressible optically thin fluid in the presence of radiation effects has been investigated. The governing boundary layer equations are first transformed into a non-dimensional form and the resulting nonlinear system of partial differential equations are then solved numerically using a very efficient finite-difference method known as the Keller-box scheme. Here we have focused our attention on the evolution of the shear stress in terms of local skin friction and the rate of heat transfer in terms of local Nusselt number, velocity profiles as well as temperature profiles for some selected values of parameter sets consisting of heat generation parameter Q, radiation parameter Rd, surface temperature parameter θ_w and the Prandlt number Pr.

2.2 Formulation of the problem

Natural convection boundary layer flow on a sphere of radius a of a steady two dimensional viscous incompressible fluid in presence of heat generation and radiation heat transfer has been investigated. It is assumed that the surface temperature of the sphere, T_w, is constant, where $T_w > T_\infty$. Here T_∞ is the ambient temperature of the fluid, T is the temperature of the fluid in the boundary layer, g is the acceleration dne to gravity, $r(\hat{x})$ is the radial distance from the symmetrical axis to the surface of the sphere and $(\hat{u}, \hat{v})$ are velocity components along the $(\hat{x}, \hat{y})$ axes. The physical configuration considered is as shown in Fig.2.1:

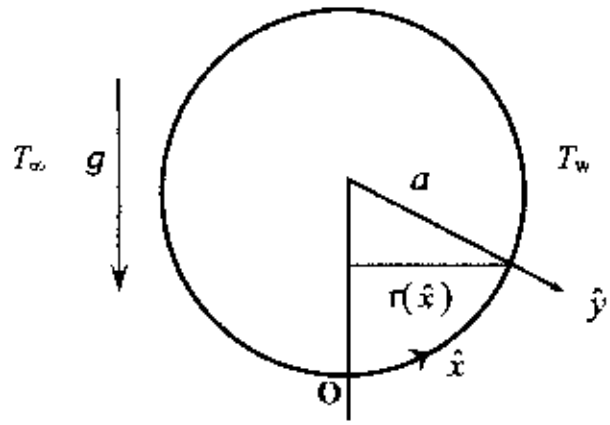

Fig.2.1: Physical model and coordinate system

Under the usual Boussinesq and boundary layer approximation, the equations for continuity, momentum and energy take the following form:

$$\frac{\partial}{\partial \hat{x}}(r\hat{u}) + \frac{\partial}{\partial \hat{y}}(r\hat{v}) = 0 \tag{2.1}$$

$$\hat{u}\frac{\partial \hat{u}}{\partial \hat{x}} + \hat{v}\frac{\partial \hat{u}}{\partial \hat{y}} = \upsilon\frac{\partial^2 \hat{u}}{\partial \hat{y}^2} + g\beta\left(T - T_\infty\right)\sin\left(\frac{\hat{x}}{a}\right) \tag{2.2}$$

$$\hat{u}\frac{\partial T}{\partial \hat{x}} + \hat{v}\frac{\partial T}{\partial \hat{y}} = \frac{k}{\rho c_p}\left(\frac{\partial^2 T}{\partial \hat{y}^2} - \frac{1}{k}\frac{\partial q_r}{\partial \hat{y}}\right) + \frac{Q_0}{\rho c_p}\left(T - T_\infty\right) \tag{2.3}$$

With the boundary conditions

$$\begin{aligned} &\hat{u} = \hat{v} = 0,\ T = T_w \quad \text{at} \quad \hat{y} = 0 \\ &\hat{u} \to 0,\ T \to T_\infty \quad \text{as} \quad \hat{y} \to \infty \end{aligned} \tag{2.4}$$

where $r(\hat{x})=a\sin\left(\frac{\hat{x}}{a}\right)$ (2.5)

$r(\hat{x})$ is the radial distance from the centre to the surface of the sphere, ρ is the density, k is the thermal conductivity, β is the coefficient of thermal expansion, ν is the reference kinematic viscosity $(\nu = \mu/\rho)$, μ is the viscosity of the fluid, C_p is the specific heat due to constant pressure and q_r is the radiative heat flux in the $\hat{y}$ direction. In order to reduce the complexity of the problem and to provide a means of comparison with future studies that will employ a more detail representation for the radiative heat flux, we will consider the optically thick radiation limit. Thus radiation heat flux term is simplified by the Rosseland diffusion approximation [Özisik (1973)] and is given by

$$q_r = -\frac{4\sigma}{3(a_r+\sigma_s)}\frac{\partial T^4}{\partial \hat{y}} \tag{2.6}$$

In Equation (2.6) a_r is the Rosseland mean absorption co-efficient, σ_s is the scattering co-efficient and σ is the Stephan-Boltzman constant.

Now introduce the following non-dimensional variables:

$$x=\frac{\hat{x}}{a},\ y=Gr^{1/4}\left(\frac{\hat{y}}{a}\right),\quad u=\frac{a}{\upsilon}Gr^{-1/2}\hat{u},\quad v=\frac{a}{\upsilon}Gr^{-1/4}\hat{v}, \tag{2.7}$$

$$\theta=\frac{T-T_\infty}{T_w-T_\infty},\qquad Gr=\frac{g\beta(T_w-T_\infty)a^3}{\upsilon^2} \tag{2.8}$$

$$\theta_w=\frac{T_w}{T_\infty},\ \Delta=\theta_w-1=\frac{T_w}{T_\infty}-1=\frac{T_w-T_\infty}{T_\infty},\ Rd=\frac{4\sigma T_\infty^3}{k(a+\sigma_s)} \tag{2.9}$$

where Gr is the Grashof number, θ is the non-dimensional temperature function, θ_w is the surface temperature parameter and Rd is the radiation parameter.

Substituting (2.7), (2.8) and (2.9) into Equations (2.1), (2.2) and (2.3) leads to the following non-dimensional equations

$$\frac{\partial}{\partial x}(ru)+\frac{\partial}{\partial y}(rv)=0 \tag{2.10}$$

$$u\frac{\partial u}{\partial x}+v\frac{\partial u}{\partial y}=\frac{\partial^2 u}{\partial y^2}+\theta\sin x \tag{2.11}$$

$$u\frac{\partial\theta}{\partial x}+v\frac{\partial\theta}{\partial y}=\frac{1}{Pr}\frac{\partial}{\partial y}\left[\left\{1+\frac{4}{3}Rd\left(1+(\theta_w-1)\theta\right)^3\right\}\frac{\partial\theta}{\partial y}\right]+Q\theta \tag{2.12}$$

where $Pr=\frac{\upsilon c_p}{k}$ is the Prandtl number and $Q=\frac{Q_o a^2}{\mu c_p Gr^{1/2}}$ is the heat generation parameter.

With the boundary conditions (2.4) become

$$\begin{aligned} &u=v=0,\quad \theta=1 \quad \text{at} \quad y=0\\ &u\to 0,\quad \theta\to 0 \quad \text{as} \quad y\to\infty \end{aligned} \tag{2.13}$$

To solve Equations (2.11) and (2.12) with the help of following variables

$$\psi=xr(x)f(x,y),\quad \theta=\theta(x,y),\quad r(x)=\sin x \tag{2.14}$$

where ψ is the stream function defined by

$$u=\frac{1}{r}\frac{\partial\psi}{\partial y},\quad v=-\frac{1}{r}\frac{\partial\psi}{\partial x} \tag{2.15}$$

Then

$$u=\frac{1}{r}\frac{\partial\psi}{\partial y}=\frac{1}{r}\frac{\partial}{\partial y}(xrf)=xf',\quad where\ f'=\frac{\partial f}{\partial y}$$

$$\frac{\partial u}{\partial x}=x\frac{\partial f'}{\partial x}+f',\quad \frac{\partial u}{\partial y}=xf'',\quad \frac{\partial^2 u}{\partial y^2}=xf'''$$

$$u\frac{\partial u}{\partial x}=xf'(x\frac{\partial f'}{\partial x}+f')=x^2f'\frac{\partial f'}{\partial x}+xf'^2$$

$$v=-\frac{1}{r}\frac{\partial\psi}{\partial x}=-\frac{1}{r}\frac{\partial}{\partial x}(xrf)=-\frac{1}{r}(rf+xr'f+xr\frac{\partial f}{\partial x})=-f-\frac{\cos x}{\sin x}xf-x\frac{\partial f}{\partial x}$$

$$v\frac{\partial u}{\partial y}=(-f-\frac{\cos x}{\sin x}xf-x\frac{\partial f}{\partial x})xf''=-xff''-\frac{\cos x}{\sin x}x^2ff''-x^2f''\frac{\partial f}{\partial x}$$

Equation (2.11) becomes

$$x^2 f'\frac{\partial f'}{\partial x} + xf'^2 - xff'' - \frac{\cos x}{\sin x}x^2 ff'' - x^2 f''\frac{\partial f}{\partial x} = xf''' + \theta \sin x$$

$$\frac{\partial^3 f}{\partial y^3} + \left(1 + \frac{1}{\sin x}x\cos x\right) f\frac{\partial^2 f}{\partial y^2} + \frac{\theta}{x}\sin x - \left(\frac{\partial f}{\partial y}\right)^2 = x\left(\frac{\partial f}{\partial y}\frac{\partial^2 f}{\partial x \partial y} - \frac{\partial f}{\partial x}\frac{\partial^2 f}{\partial y^2}\right) \tag{2.16}$$

Equation (2.12) becomes

$$xf'\frac{\partial \theta}{\partial x} + \left(-f - \frac{\cos x}{\sin x}xf - x\frac{\partial f}{\partial x}\right)\frac{\partial \theta}{\partial y} = \frac{1}{Pr}\frac{\partial}{\partial y}\left\{\left(1 + \frac{4}{3}Rd(1 + (\theta_w - 1)\theta)^3\right)\frac{\partial \theta}{\partial y}\right\} + Q\theta$$

$$\frac{1}{Pr}\frac{\partial}{\partial y}\left\{\left(1 + \frac{4}{3}Rd(1 + (\theta_w - 1)\theta)^3\right)\frac{\partial \theta}{\partial y}\right\} + \left(1 + \frac{x}{\sin x}\cos x\right) f\frac{\partial \theta}{\partial y} + Q\theta = x\left(\frac{\partial f}{\partial y}\frac{\partial \theta}{\partial x} - \frac{\partial \theta}{\partial y}\frac{\partial f}{\partial x}\right) \tag{2.17}$$

Along with boundary conditions

$$\begin{aligned} &f = f' = 0, \quad \theta = 1 \qquad \text{at} \quad y = 0 \\ &f' \to 0, \quad \theta \to 0 \quad \text{as} \quad y \to \infty \end{aligned} \tag{2. 18}$$

where primes denote differentiation of the function with respect to y.

It can be seen that near the lower stagnation point of the sphere i.e. $x \approx 0$, Equations (2.16) and (2.17) reduce to the following ordinary differential equations:

$$f''' + 2ff'' - f'^2 + \theta = 0 \tag{2.19}$$

$$\frac{1}{Pr}\left[\left\{1 + \frac{4}{3}Rd(1 + (\theta_w - 1)\theta)^3\right\}\theta'\right]' + 2f\theta' + Q\theta = 0 \tag{2.20}$$

Subject to the boundary conditions

$$\begin{aligned} &f(0) = f'(0) = 0, \quad \theta(0) = 1 \\ &f' \to 0, \quad \theta \to 0 \quad \text{as} \quad y \to \infty \end{aligned} \tag{2.21}$$

In practical applications, the physical quantities of principle interest are the shearing stress τ_w and the rate of heat transfer in terms of the skin-friction coefficients C_{fx} and Nusselt number Nu_x respectively, which can be written as

$$Nu_x = \frac{aGr^{-1/4}}{k(T_w - T_\infty)}(q_c + q_r)_{\hat{y}=0} \text{ and } \quad C_{f_x} = \frac{Gr^{-3/4}a^2}{\mu_\infty \upsilon_\infty}(\tau_w)_{\hat{y}=0} \tag{2.22}$$

where $\tau_w = \mu\left(\frac{\partial \hat{u}}{\partial \hat{y}}\right)_{\hat{y}=0}$ and $q_c = -k\left(\frac{\partial T}{\partial \hat{y}}\right)_{\hat{y}=0}$, q_c is the conduction heat flux. (2.23)

Using the Equations (2.8),(2.15) and the boundary condition (2.21) into (2.22) and (2.23),we get

$$C_{f_x} = xf''(x,0) \tag{2.24}$$

$$Nu_x = -\left(1 + \frac{4}{3}Rd\theta_w^3\right)\theta'(x,0) \tag{2.25}$$

The values of the velocity and temperature distribution are calculated respectively from the following relations:

$$u = x\frac{\partial f}{\partial y}, \quad \theta = \theta(x,y) \tag{2.26}$$

2.3 Results and discussion

Here we have investigated the effect of radiation on natural convection flow on a sphere in presence of heat generation. Solutions are obtained for fluids having Prandtl number Pr = 0.72 (air) and for some test values of Pr = 2.0, 3.0 and 4.0 against y for a wide range of values of radiation parameter Rd, surface temperature parameter θ_w and heat generation parameter Q. We have considered the values of heat generation parameter Q = 0.2, 0.3, 0.5 and 0.6 with radiation parameter Rd=1.0, Prandtl number Pr = 0.72 and surface temperature parameter θ_w = 1.1. The values of radiation parameter Rd =1.0, 1.5, 2.0, 2.5 and 3.0 have been taken while Q = 0.5, Pr = 0.72 and θ_w = 1.1. Different values of surface temperature parameter θ_w = 0.1, 0.4, 0.8, 1.3 and 1.6 are considered while Q = 0.4, Pr = 0.72 and Rd =1.0. Numerical values of local rate of heat transfer are calculated in terms of Nusselt number Nu for the surface of the sphere from lower stagnation point to upper stagnation point. The effect for different values of heat generation parameter Q on local skin friction coefficient C_f and the local Nusselt number Nu, as well as velocity and temperature profiles

with the Prandtl number Pr = 0.72, radiation parameter Rd =1.0 and surface temperature parameter θ_w = 1.1.

Figures 2.1-2.2 display results for the velocity and temperature profiles, for different values of heat generation parameter Q with Prandtl number Pr = 0.72, radiation parameter Rd =1.0 and surface temperature parameter θ_w = 1.1. It has been seen from Figures 2.1 and 2.2 that as the heat generation parameter Q increases, the velocity and the temperature profiles increase. The changes of velocity profiles in the y direction reveals the typical velocity profile for natural convection boundary layer flow, i.e., the velocity is zero at the boundary wall then the velocity increases to the peak value as y increases and finally the velocity approaches to zero (the asymptotic value).The maximum values of velocity are recorded to be 0.47717, 0.49274, 0.52815 and 0.54807 for Q=0.2, 0.3, 0.5 and 0.6 respectively which occur at the same point y = 1.23788. Here, it is observed that at y = 1.23788, the velocity increases by 12.839% as the heat generation parameter Q changes from 0.2 to 0.6. The changes of temperature profiles in the y direction also shows the typical temperature profile for natural convection boundary layer flow that is the value of temperature profile is 1.0 (one) at the boundary wall then the temperature profile decreases gradually along y direction to the asymptotic value.

The effect for different values of radiation parameter Rd the velocity and temperature profiles in case of Prandtl number Pr = 0.72, heat generation parameter Q = 0.5 and surface temperature parameter θ_w = 1.1 are shown in Figures 2.3 and 2.4. Here, radiation parameter Rd increases, the velocity profile increases and the temperature profile increases slightly such that there exists a local maximum of the velocity within the boundary layer, but velocity increases near the surface of the sphere and then temperature decreases slowly and finally approaches to zero.

The effect of different values of surface temperature parameterθ_w, the velocity and temperature profiles while Prandtl number Pr = 0.72, heat generation parameter Q = 0.4 and radiation parameter Rd =1.0 are shown in Figures 2.5 and 2.6. Here, as surface temperature parameter θ_w increases, the velocity profile increases and the temperature profile increases such that there exists a local maximum of the velocity within the boundary layer, but velocity increases near the surface of the sphere and then temperature decreases slowly and

finally approaches to zero. However, in Figures 2.7 and 2.8, it is shown that when the Prandtl number Pr increases with θ_w = 1.1, Rd =1.0 and Q = 0.5, both the velocity and temperature profiles decrease.

Figures 2.9-2.10 show that skin friction coefficient C_f increases and heat transfer coefficient Nu decreases respectively for increasing values of heat generation parameter Q. in case of Prandtl number Pr = 0.72, radiation parameter Rd =1.0 and surface temperature parameter θ_w = 1.1. The values of skin friction coefficient C_f and Nusselt number Nu are recorded to be 1.10630, 1.13520, 1.19701, 1.23286 and 0.46402, 0.28301, 0.06937, -0.08860 for Q=0.2, 0.3, 0.5, 0.6 respectively which occur at the same point x = 1.57080. Here, it is observed that at x = 1.57080, the skin friction increases by 10.265% and Nusselt number Nu decreases by 119.094% as the heat generation parameter Q changes from fl.2 to 0.6. It is observed from the figure 2.9 that the skin friction increases gradually from zero value at lower stagnation point along the x direction and from Figure 2.10, it reveals that the rate of heat transfer decreases along the x direction from lower stagnation point to the upstream.

The effect of different values of radiation parameter Rd on the skin friction coefficient and the local rate of heat transfer while Prandtl number Pr = 0.72, heat generation parameter Q = 0.5 and surface temperature parameter θ_w = 1.1 are shown in the figures 2.11- 2.12. Here, as the radiation parameter Rd increases, both the skin friction coefficient and heat transfer coefficient increase.

From Figures 2.13 - 2.14, it can also easily be seen that an increase in the surface temperature parameter θ_w leads to increase in the local skin friction coefficient C_f and the local rate of heat transfer Nu while Prandtl number Pr = 0.72, heat generation parameter Q = 0.4 and radiation parameter Rd =1.0. It is also observed that at any position of x, the skin friction coefficient C_f and the local Nusselt number Nu increase as θ_w increases from 0.1 to 1.6. This phenomenon can easily be understood from the fact that when the surface temperature parameter θ_w increases, the temperature of the fluid rises and the thickness of the velocity boundary layer grows, i.e., the thermal boundary layer becomes thinner than the velocity boundary layer. Therefore the skin friction coefficient C_f and the local Nusselt number Nu increase.

The variation of the local skin friction coefficient C_f and local rate of heat transfer Nu for different values of Prandtl number Pr for $\theta_w = 1.1$, $Rd = 1.0$ and $Q = 0.5$ are shown in Figures 2.15 and 2.16. We can observe from these figures that as the Prandtl number Pr increases, both the skin friction coefficient and rate of heat transfer decrease but the rate of increase in the rate of heat transfer are higher than that of the skin friction coefficient. So, the effect of Prandtl number Pr on the rate of heat transfer is more than that of the effect of Prandtl number Pr on skin friction coefficient.

Numerical values of skin friction coefficient C_f and rate of heat transfer Nu are calculated from equations (2.24) and (2.25) for the surface of the sphere from lower stagnation point at $x = 0^0$ to $x = 90^0$. Numerical values of C_f and Nu are depicted in Table 2.1.

Table 2. 1: Skin friction coefficient and rate of heat transfer against x for different values of heat generation parameter Q with other controlling parameters $Pr = 0.72$, $Rd = 1.0$, $\theta_w = 1.1$.

	$Q = 0.2$		$Q = 0.3$		$Q = 0.5$		$Q = 0.6$	
x	C_f	Nu	C_f	Nu	C_f	Nu	C_f	Nu
0.00000	0.00000	0.65680	0.00000	0.55338	0.00000	0.32045	0.00000	0.18834
0.10472	0.09608	0.65592	0.09811	0.55243	0.10269	0.31932	0.10529	0.18709
0.20944	0.19153	0.65342	0.19557	0.54972	0.20474	0.31609	0.20993	0.18354
0.31416	0.28571	0.64931	0.29177	0.54526	0.30551	0.31076	0.31329	0.17767
0.40143	0.36280	0.64464	0.37053	0.54019	0.38806	0.30471	0.39798	0.17100
0.50615	0.45310	0.63752	0.46282	0.53247	0.48487	0.29548	0.49736	0.16083
0.61087	0.54043	0.62875	0.55212	0.52295	0.57866	0.28409	0.59369	0.14828
0.71558	0.62421	0.61828	0.63785	0.51158	0.66882	0.27050	0.68637	0.13329
0.80285	0.69090	0.60824	0.70614	0.50069	0.74075	0.25745	0.76038	0.11891
0.90757	0.76668	0.59459	0.78381	0.48586	0.82274	0.23969	0.84481	0.09932
1.01229	0.83734	0.57914	0.85631	0.46907	0.89946	0.21957	0.92394	0.07712
1.20428	0.95180	0.54599	0.97402	0.43303	1.02460	0.17633	1.05331	0.02941
1.57080	1.10630	0.46402	1.13396	0.34388	1.19701	0.06937	1.23286	-0.08860

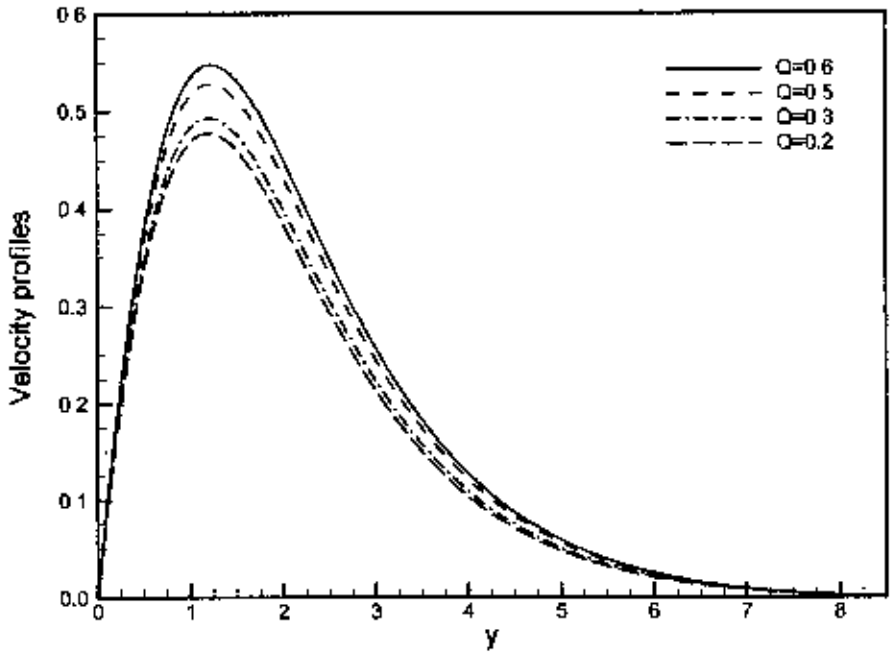

Figure 2.1: Velocity profiles for different values of Q with $Pr = 0.72$, $Rd = 1.0$ and $\theta_w = 1.1$

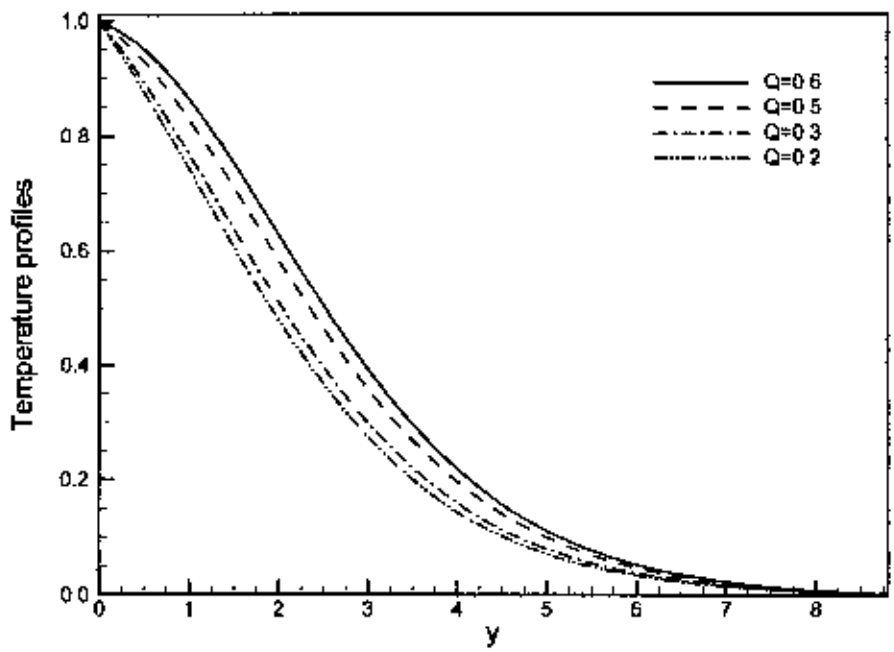

Figure 2.2: Temperature profiles for different values of Q with $Pr = 0.72$, $Rd = 1.0$ and $\theta_w = 1.1$

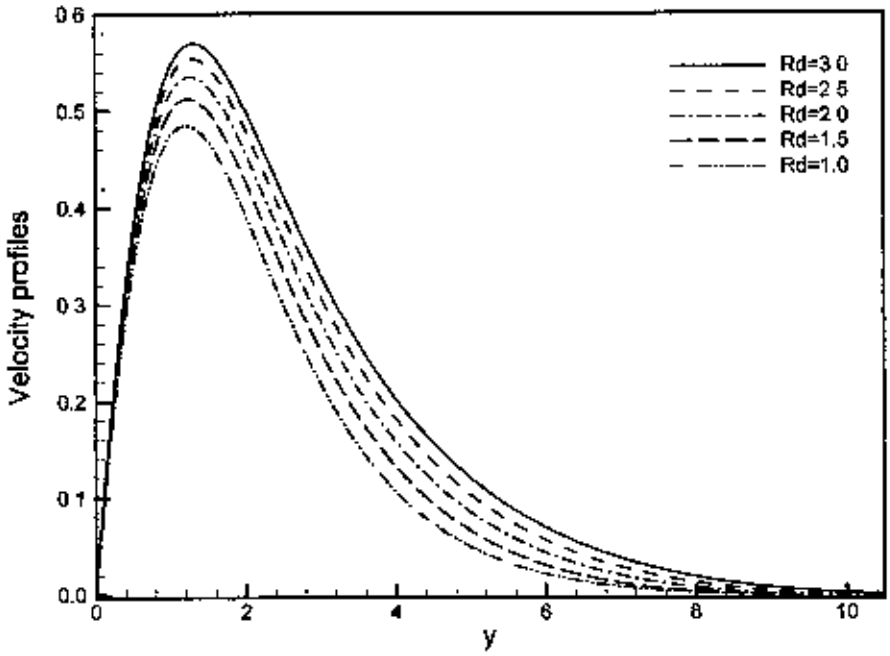

Figure 2.3: Velocity profiles for different values of *Rd* with $Pr = 0.72$, $\theta_w = 1.1$ and $Q=0.5$

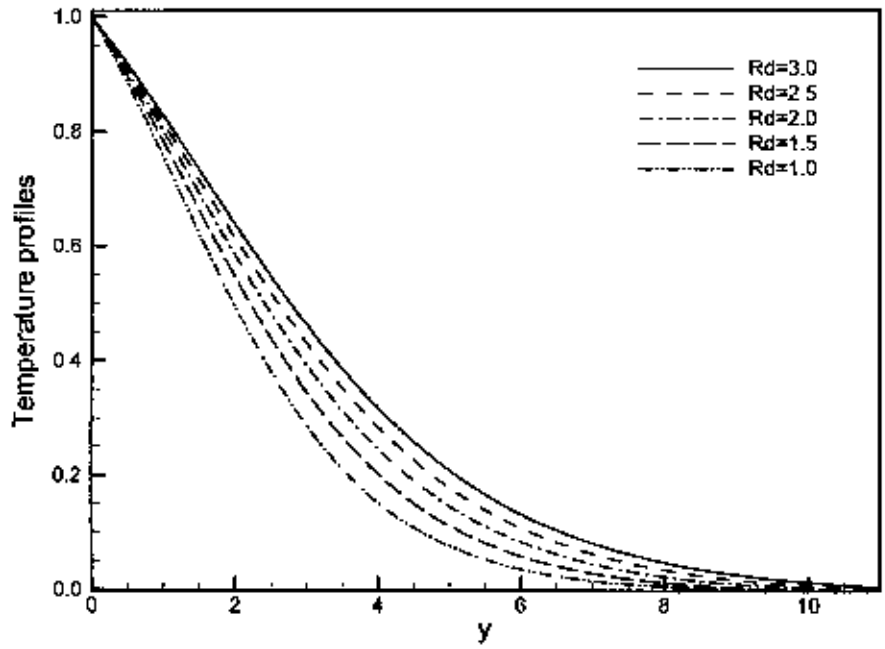

Figure 2.4: Temperature profiles for different values *Rd* with $Pr = 0.72$, $\theta_w = 1.1$ and $Q=0.5$

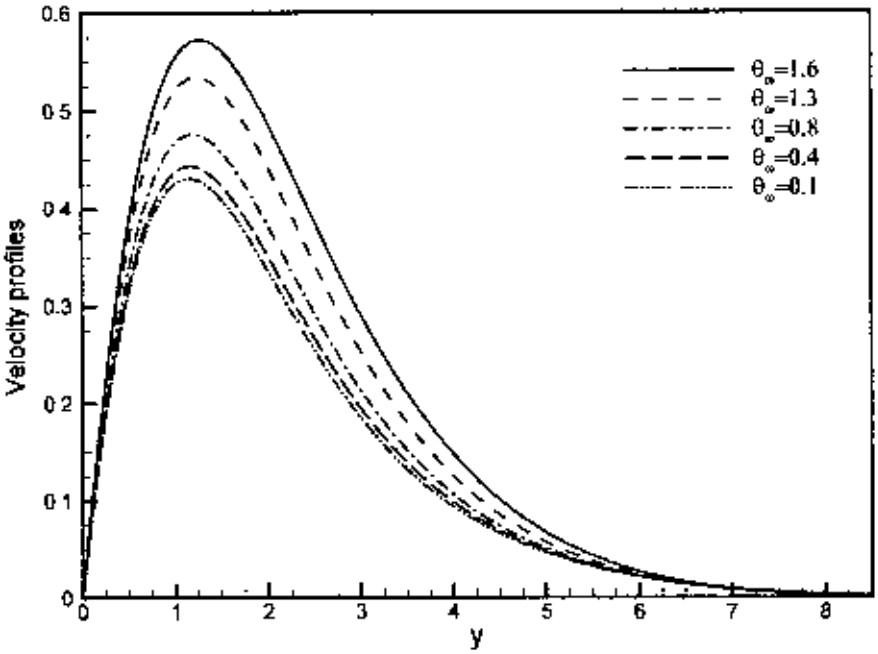

Figure 2.5: Velocity profiles for different values of θ_w with $Pr = 0.72$, $Rd = 1.0$ and $Q = 0.4$

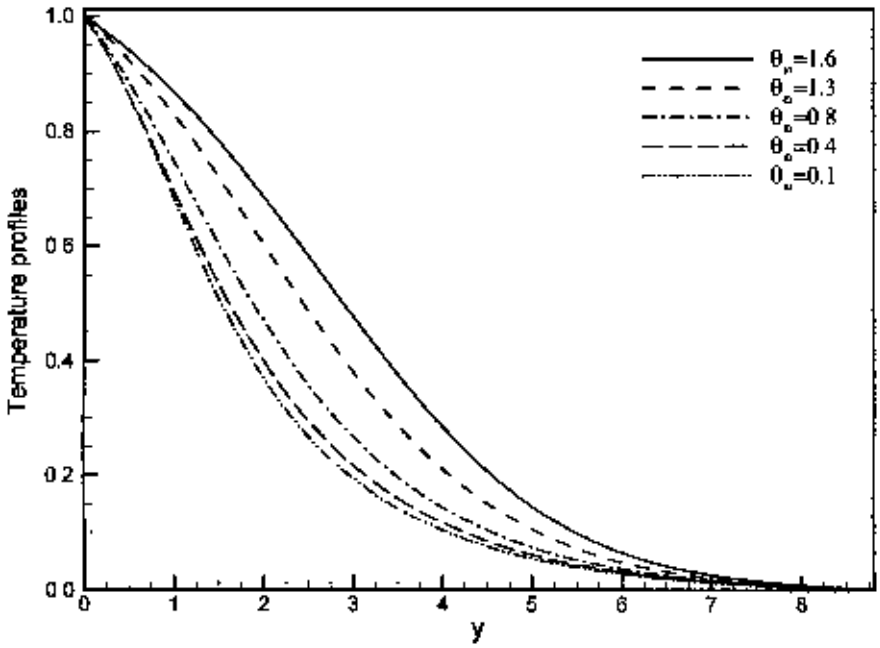

Figure 2.6: Temperature profiles for different values of θ_w with $Pr = 0.72$, $Rd = 1.0$ and $Q = 0.4$

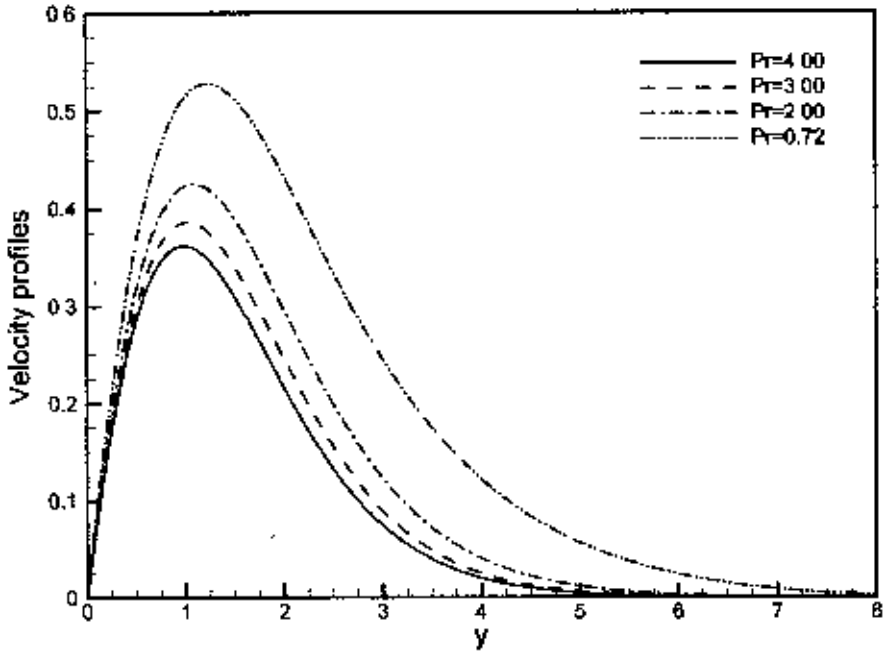

Figure 2.7: Velocity profiles for different values of Pr with Rd=1.0, θ_w=1.1 and Q=0.5

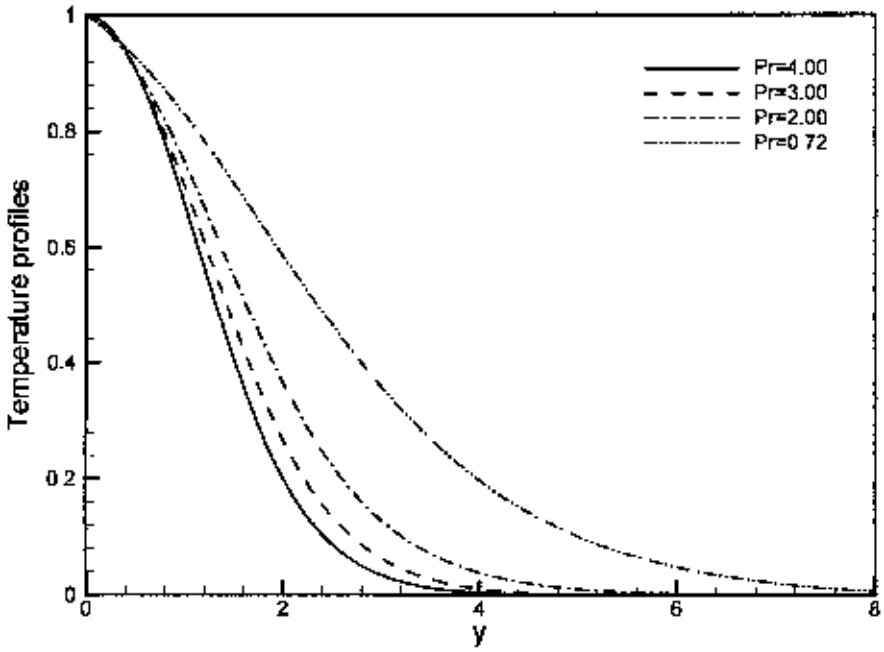

Figure 2.8: Temperature profiles for different values of Pr with Rd=1.0, θ_w=1.1, and Q=0.5

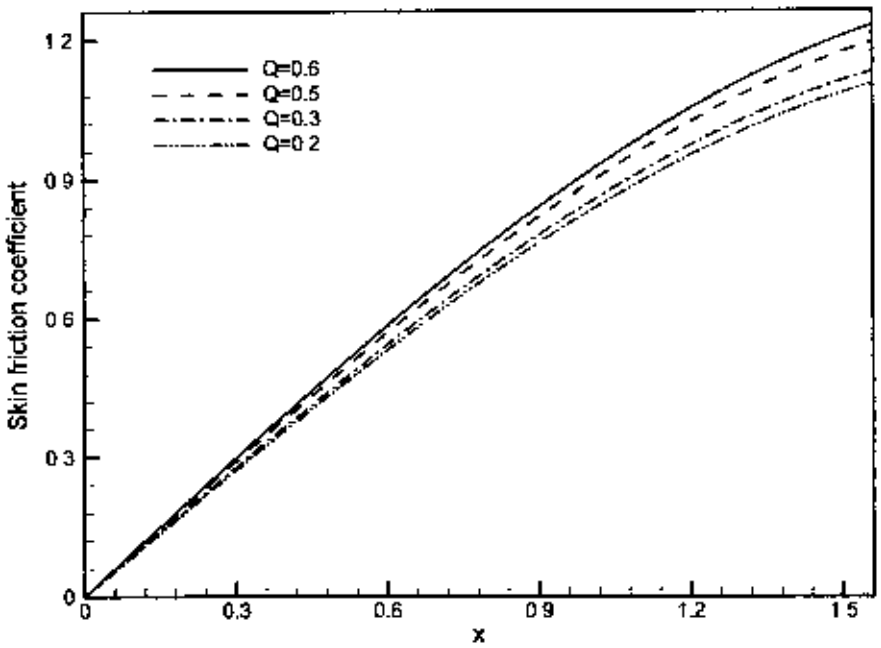

Figure 2.9: Skin-friction coefficient for different values of Q with $Pr = 0.72$, $Rd = 1.0$, and $\theta_w = 1.1$

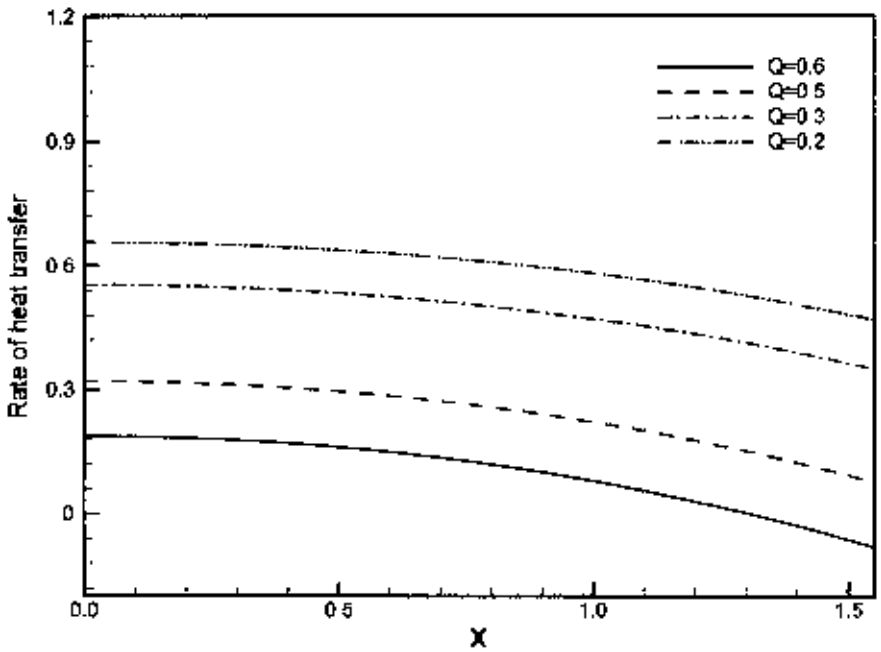

Figure 2.10: Rate of heat transfer for different values of Q with $Pr = 0.72$, $Rd = 1.0$, $\theta_w = 1.1$

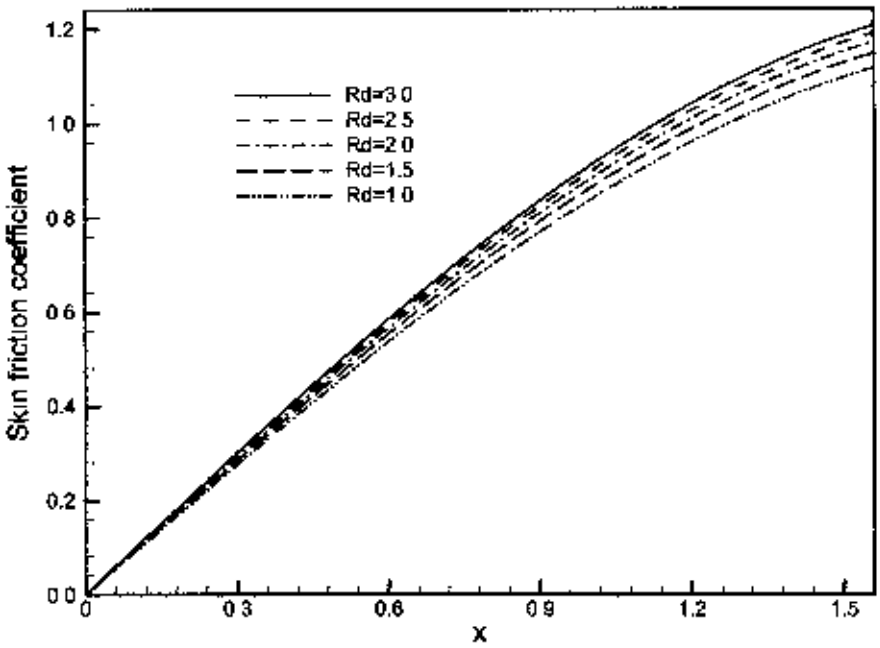

Figure 2.11: Skin-friction coefficient for different values of Rd with $Pr = 0.72$, $\theta_w = 1.1$ and $Q=0.5$

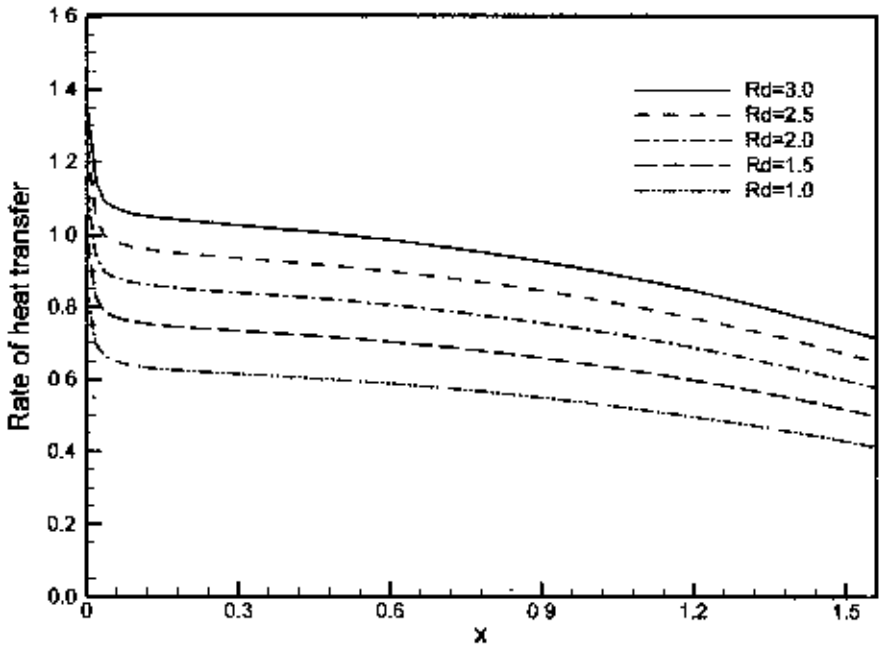

Figure 2.12: Rate of heat transfer for different values of Rd with $Pr = 0.72$, $\theta_w = 1.1$ and $Q=0.5$

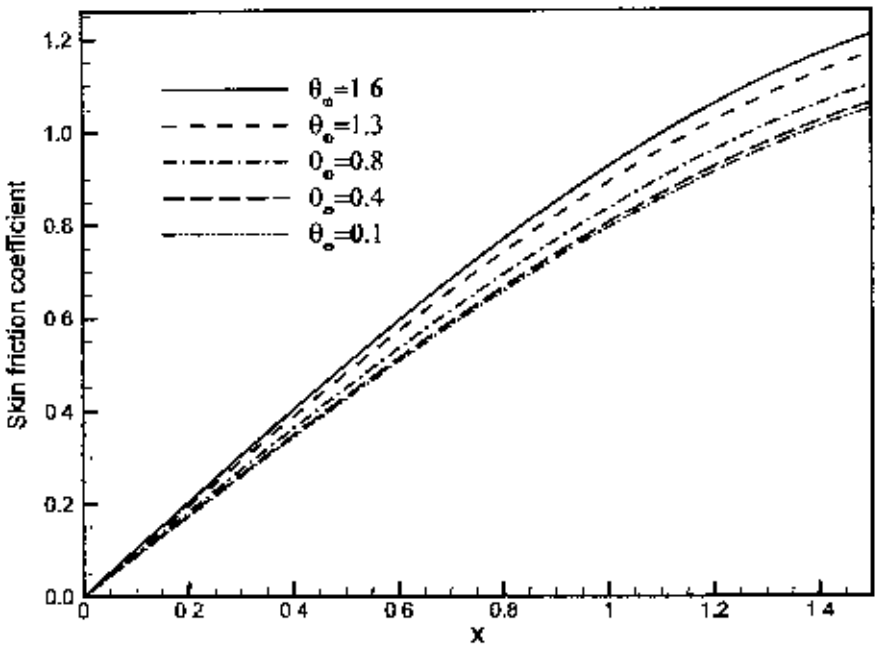

Figure 2.13: Skin-friction coefficient for different values of θ_w with $Pr = 0.72$, $Rd = 1.0$ and $Q = 0.4$

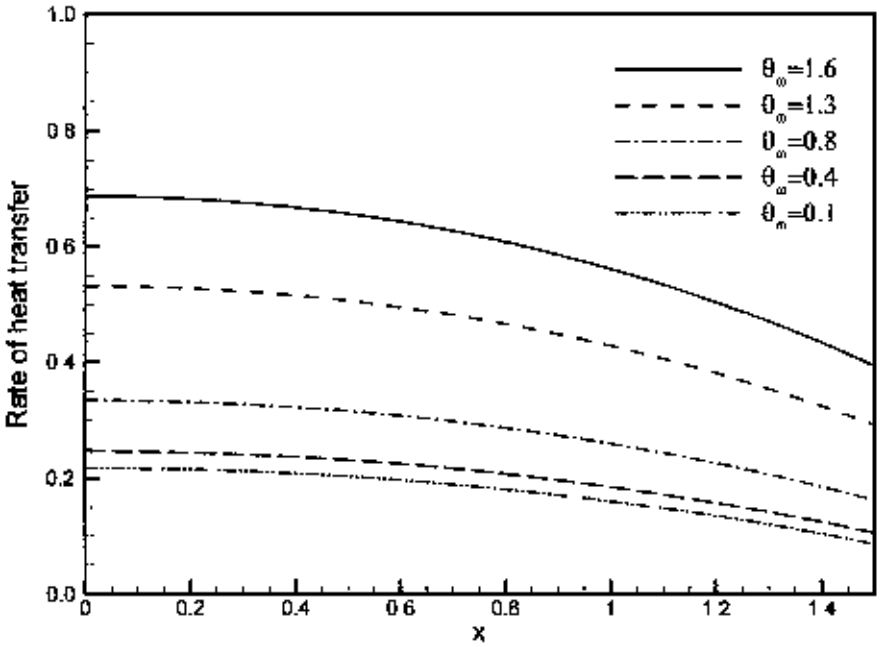

Figure 2.14: Rate of heat transfer for different values of θ_w with $Pr = 0.72$, $Rd = 1.0$ and $Q = 0.4$

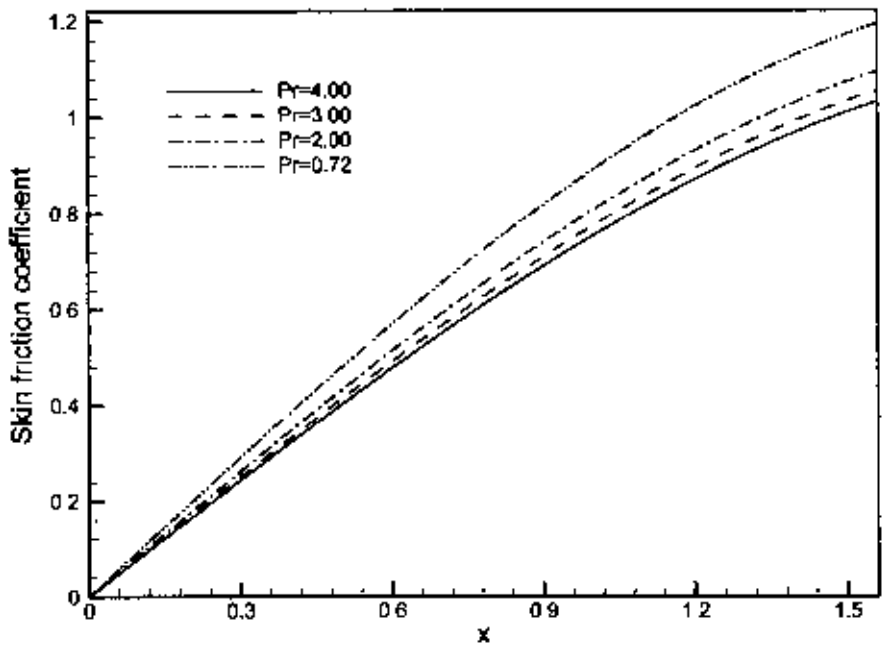

Figure 2.15: Skin-friction coefficient for different values of Pr with Rd =1.0, θ_w =1.1 and Q=0.5

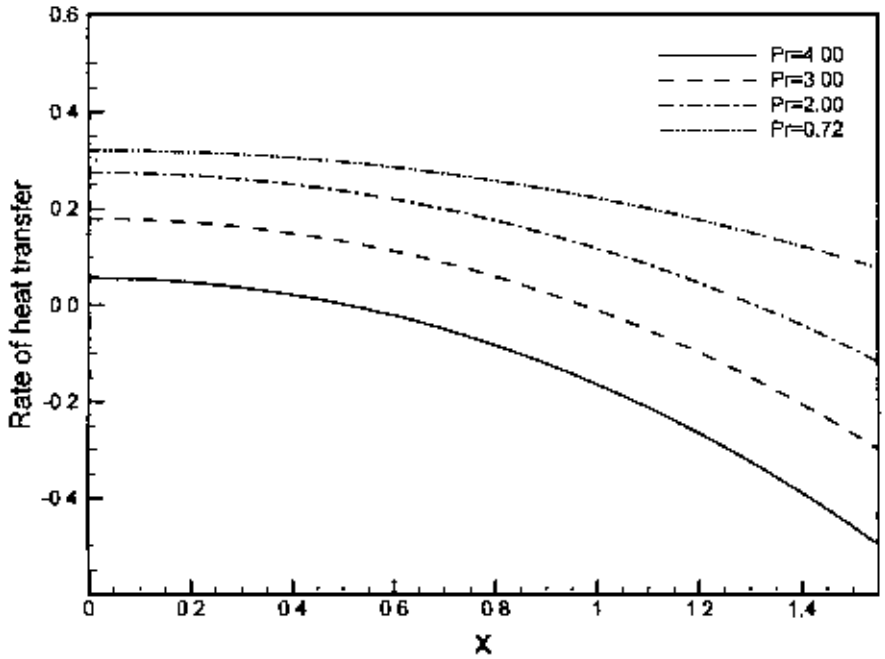

Figure 2.16: Rate of heat transfer for different values of Pr with Rd =1.0, θ_w =1.1 and Q=0.5

2.4 Conclusion

The effect of radiation on natural convection flow on a sphere in presence of heat generation has been investigated for different values of relevant physical parameters including Prandtl number Pr, and surface temperature parameter θ_w.

The governing boundary layer equations of motion are transformed into a non-dimensional form and the resulting non-linear systems of partial differential equations are reduced to local non-similarity boundary layer equations, which are solved numerically by using implicit finite difference method together with the Keller-box scheme. From the present investigation, following conclusions may be drawn:

- Significant effects of heat generation parameter Q on velocity and temperature profiles as well as on skin friction and the rate of heat transfer have been found in this investigation but the effect of heat generation parameter Q on rate of heat transfer is more significant. An increase in the values of heat generation parameter Q leads to increase both the velocity and the temperature profiles, the local skin friction coefficient C_f increases at different position of y but the local rate of heat transfer Nu decreases at different position of x for Pr =0.72.
- The increase in the values of radiation parameter Rd leads to increase in the velocity profile, the temperature profile, the local skin friction coefficient C_f and the local rate of heat transfer Nu.
- All the velocity profile, temperature profile, the local skin friction coefficient C_f and the local rate of heat transfer Nu increase significantly when the values of surface temperature parameter θ_w increase.
- The increase in Prandtl number Pr leads to decrease in all the velocity profile, the temperature profile, the local skin friction coefficient C_f and the local rate of heat transfer Nu.

Chapter 3

Effect of Radiation on Magnetohydrodynamic Natural Convection Flow on a Sphere in Presence of Heat Generation

3.1 Introduction

In this chapter, the description of the effect of radiation on magnetohydrodynamic (MHD) natural convection flow on a sphere in presence of heat generation has been focused. The governing boundary layer equations are first transformed into a non-dimensional form and the resulting nonlinear system of partial differential equations are then solved numerically using a very efficient finite-difference method known as the Keller-box scheme. Here the attention has given on the evolution of the surface shear stress in terms of local skin friction and the rate of heat transfer in terms of local Nusselt number, velocity distribution as well as temperature distribution for a selection of parameter sets consisting of heat generation parameter, magnetohydrodynamic (MHD) parameter and the Prandlt number.

3.2 Formulation of the problem

A steady two-dimensional magnetohydrodynamic (MHD) natural convection boundary layer flow from an isothermal sphere of radius a, which is immersed in a viscous and incompressible optically dense fluid with heat generation and radiation heat loss is considered. It is assumed that the surface temperature of the sphere, T_w, is constant, where $T_w > T_\infty$. Here T_∞ is the ambient temperature of the fluid, T is the temperature of the fluid in the boundary layer, g is the acceleration due to gravity, $r(\hat{x})$ is the radial distance from the symmetrical axis to the surface of the sphere and $(\hat{u}, \hat{v})$ are velocity components along the $(\hat{x}, \hat{y})$ axes. The physical configuration considered is as shown in Fig. 3.1:

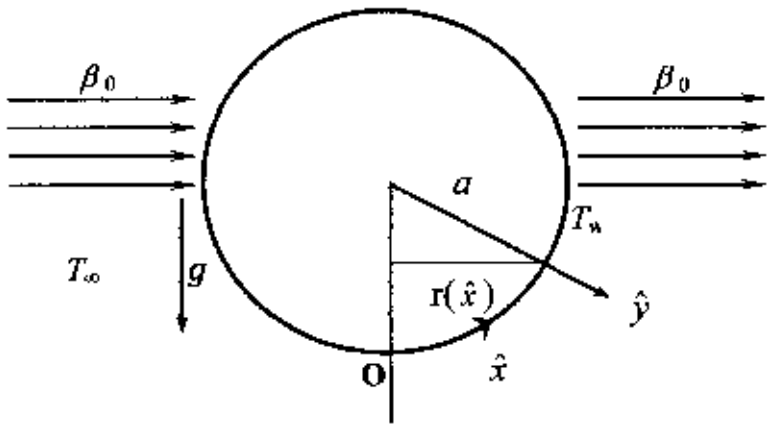

Fig. 3.1: Physical model and coordinate system

Under the above assumptions, the governing equations for steady two-dimensional laminar boundary layer flow problem under consideration can be written as

$$\frac{\partial}{\partial \hat{x}}(r\,\hat{u}) + \frac{\partial}{\partial \hat{y}}(r\hat{v}) = 0 \tag{3.1}$$

$$\hat{u}\frac{\partial \hat{u}}{\partial \hat{x}} + \hat{v}\frac{\partial \hat{u}}{\partial \hat{y}} = \upsilon\frac{\partial^2 \hat{u}}{\partial \hat{y}^2} + g\beta(T - T_\infty)\sin\left(\frac{\hat{x}}{a}\right) - \frac{\sigma_0 \beta_0^{\,2}}{\rho}\hat{u} \tag{3.2}$$

$$\hat{u}\frac{\partial T}{\partial \hat{x}} + \hat{v}\frac{\partial T}{\partial \hat{y}} = \frac{k}{\rho c_p}\left(\frac{\partial^2 T}{\partial \hat{y}^2} - \frac{1}{k}\frac{\partial q_r}{\partial \hat{y}}\right) + \frac{Q_o}{\rho c_p}(T - T_\infty) \tag{3.3}$$

With the boundary conditions

$$\hat{u} = \hat{v} = 0,\ T = T_w \ at\ \hat{y} = 0$$
$$\hat{u} \to 0,\ T \to T_\infty \ as\ \hat{y} \to \infty \tag{3.4}$$

where $r(\hat{x}) = a\sin\left(\frac{\hat{x}}{a}\right)$ (3.5)

$r(\hat{x})$ is the radial distance from the centre to the surface of the sphere, g is the acceleration due to gravity, ρ is the density, k is the thermal conductivity, β is the coefficient of thermal expansion, β_0 is the strength of magnetic field, σ_0 is the electrical conduction, ν is the reference kinematic viscosity, μ is the viscosity of the fluid, C_p is the specific heat due to constant pressure.

The above equations are further non-dimensionalised using the new variables:

$$x = \frac{\hat{x}}{a},\ y = Gr^{1/4}\left(\frac{\hat{y}}{a}\right),\quad u = \frac{a}{\upsilon}Gr^{-1/2}\hat{u},\quad v = \frac{a}{\upsilon}Gr^{-1/4}\hat{v}, \tag{3.6}$$

$$\theta = \frac{T - T_\infty}{T_w - T_\infty},\qquad Gr = \frac{g\beta(T_w - T_\infty)a^3}{\upsilon^2} \tag{3.7}$$

$$\theta_w = \frac{T_w}{T_\infty},\ \Delta = \theta_w - 1 = \frac{T_w}{T_\infty} - 1 = \frac{T_w - T_\infty}{T_\infty},\ Rd = \frac{4\sigma T_\infty^3}{k(a + \sigma_s)} \tag{3.8}$$

where Gr is the Grashof number, θ is the non-dimensional temperature function, T_w is the constant temperature at the surface , θ_w is the surface temperature parameter and Rd is the radiation-conduction parameter.

The radiation heat flux is in the following form

$$q_r = -\frac{4\sigma}{3(a_r + \sigma_s)}\frac{\partial T^4}{\partial \hat{y}} \tag{3.9}$$

where a_r is the Rosseland mean absorption co-efficient, σ_s is the scattering co-efficient and σ is the Stephan-Boltzman constant.

Substituting (3.6), (3.7) and (3.8) into Equations (3.1), (3.2) and (3.3) leads to the following non-dimensional equations

$$\frac{\partial}{\partial x}(ru) + \frac{\partial}{\partial y}(rv) = 0 \tag{3.10}$$

$$u\frac{\partial u}{\partial x} + v\frac{\partial u}{\partial y} = \frac{\partial^2 u}{\partial y^2} + \theta\sin x - \frac{\sigma_0\beta_0{}^2 a^2}{\rho\upsilon Gr^{1/2}}u \tag{3.11}$$

$$u\frac{\partial\theta}{\partial x}+v\frac{\partial\theta}{\partial y}=\frac{1}{Pr}\frac{\partial}{\partial y}\left[\left\{1+\frac{4}{3}Rd\left(1+(\theta_w-1)\theta\right)^3\right\}\frac{\partial\theta}{\partial y}\right]+Q\theta \tag{3.12}$$

where $Pr=\frac{\upsilon c_p}{k}$ is the Prandtl number and $Q=\frac{Q_o a^2}{\mu c_p Gr^{1/2}}$ is the heat generation parameter.

With the boundary conditions (3.4) become

$$\begin{aligned} &u=v=0,\quad \theta=1 \quad \text{at} \quad y=0\\ &u\to 0,\quad \theta\to 0 \quad \text{as} \quad y\to\infty \end{aligned} \tag{3.13}$$

To solve Equations (3.11) and (3.12) with the help of following variables

$$\psi=xr(x)f(x,y),\quad \theta=\theta(x,y),\quad r(x)=\sin x \tag{3.14}$$

where ψ is the stream function defined by

$$u=\frac{1}{r}\frac{\partial\psi}{\partial y},\quad v=-\frac{1}{r}\frac{\partial\psi}{\partial x} \tag{3.15}$$

$$u=\frac{1}{r}\frac{\partial\psi}{\partial y}=\frac{1}{r}\frac{\partial}{\partial y}(xrf)=xf',\quad \text{where } f'=\frac{\partial f}{\partial y}$$

$$\frac{\partial u}{\partial x}=x\frac{\partial f'}{\partial x}+f',\quad \frac{\partial u}{\partial y}=xf'',\quad \frac{\partial^2 u}{\partial y^2}=xf'''$$

$$u\frac{\partial u}{\partial x}=xf'(x\frac{\partial f'}{\partial x}+f')=x^2f'\frac{\partial f'}{\partial x}+xf'^2$$

$$v=-\frac{1}{r}\frac{\partial\psi}{\partial x}=-\frac{1}{r}\frac{\partial}{\partial x}(xrf)=-\frac{1}{r}(rf+xr'f+xr\frac{\partial f}{\partial x})=-f-\frac{\cos x}{\sin x}xf-x\frac{\partial f}{\partial x}$$

$$v\frac{\partial u}{\partial y}=(-f-\frac{\cos x}{\sin x}xf-x\frac{\partial f}{\partial x})xf''=-xff''-\frac{\cos x}{\sin x}x^2ff''-x^2f''\frac{\partial f}{\partial x}$$

Equation (3.11) becomes

$$\frac{1}{r}\frac{\partial\psi}{\partial y}\frac{\partial}{\partial x}(\frac{1}{r}\frac{\partial\psi}{\partial y})-\frac{1}{r}\frac{\partial\psi}{\partial x}\frac{\partial}{\partial y}(\frac{1}{r}\frac{\partial\psi}{\partial y})=\frac{\partial^2}{\partial y^2}(\frac{1}{r}\frac{\partial\psi}{\partial y})+\theta\sin x\ -\frac{\sigma_0{\beta_0}^2a^2}{\rho\upsilon Gr^{1/2}}\frac{1}{r}\frac{\partial\psi}{\partial y}$$

$$\frac{1}{r}\frac{\partial}{\partial y}(xrf)\frac{\partial}{\partial x}(\frac{1}{r}\frac{\partial}{\partial y}(xrf))-\frac{1}{r}\frac{\partial}{\partial x}(xrf)\frac{\partial}{\partial y}(\frac{1}{r}\frac{\partial}{\partial y}(xrf))=\frac{\partial^2}{\partial y^2}(\frac{1}{r}\frac{\partial}{\partial y}(xrf))+\theta\sin x\ -\frac{\sigma_0{\beta_0}^2a^2}{\rho\upsilon Gr^{1/2}}\frac{1}{r}\frac{\partial}{\partial y}(xrf)$$

$$x\frac{\partial f}{\partial y}\frac{\partial}{\partial x}(x\frac{\partial f}{\partial y})-\frac{1}{r}\frac{\partial}{\partial x}(xrf)\frac{\partial}{\partial y}(x\frac{\partial f}{\partial y})=\frac{\partial^2}{\partial y^2}(x\frac{\partial f}{\partial y})+\theta\sin x\ -\frac{\sigma_0{\beta_0}^2a^2}{\rho\upsilon Gr^{1/2}}x\frac{\partial f}{\partial y}$$

$$x\frac{\partial f}{\partial y}\left(x\frac{\partial^2 f}{\partial x\partial y}+\frac{\partial f}{\partial y}\right)-\left(x\frac{\partial f}{\partial x}+f+\frac{1}{a\sin x}xf\frac{\partial}{\partial x}(a\sin x)\right)x\frac{\partial^2 f}{\partial y^2}=x\frac{\partial^3 f}{\partial y^3}+\theta\sin x-\frac{\sigma_0\beta_0{}^2a^2}{\mu Gr^{1/2}}x\frac{\partial f}{\partial y}$$

where $r(x)=\sin x,\ \mu=\rho\upsilon$

$$x\frac{\partial f}{\partial y}\left(x\frac{\partial^2 f}{\partial x\partial y}+\frac{\partial f}{\partial y}\right)-\left(x\frac{\partial f}{\partial x}+f+\frac{1}{a\sin x}xf\frac{\partial}{\partial x}(a\sin x)\right)x\frac{\partial^2 f}{\partial y^2}=x\frac{\partial^3 f}{\partial y^3}+\theta\sin x-\frac{\sigma_0\beta_0{}^2a^2}{\mu Gr^{1/2}}x\frac{\partial f}{\partial y}$$

where $r(x)=\sin x,\ \mu=\rho\upsilon$

$$\frac{\partial^3 f}{\partial y^3}+\left(1+\frac{1}{\sin x}x\cos x\right)f\frac{\partial^2 f}{\partial y^2}+\frac{0}{x}\sin x-\left(\frac{\partial f}{\partial y}\right)^2-M\frac{\partial f}{\partial y}=x\left(\frac{\partial f}{\partial y}\frac{\partial^2 f}{\partial x\partial y}-x\frac{\partial f}{\partial x}\frac{\partial^2 f}{\partial y^2}\right)\tag{3.16}$$

where $M=\dfrac{\sigma_0\beta_0{}^2a^2}{\mu Gr^{1/2}}$ is the MHD parameter.

Equation (3.12) becomes

$$xf'\frac{\partial\theta}{\partial x}+\left(-f-\frac{\cos x}{\sin x}xf-x\frac{\partial f}{\partial x}\right)\frac{\partial\theta}{\partial y}=\frac{1}{Pr}\frac{\partial}{\partial y}\left\{\left(1+\frac{4}{3}Rd(1+(\theta_w-1)\theta)^3\right)\frac{\partial\theta}{\partial y}\right\}+Q\theta$$

$$\frac{1}{Pr}\frac{\partial}{\partial y}\left\{\left(1+\frac{4}{3}Rd(1+(\theta_w-1)\theta)^3\right)\frac{\partial\theta}{\partial y}\right\}+\left(1+\frac{x}{\sin x}\cos x\right)f\frac{\partial\theta}{\partial y}+Q\theta=x\left(\frac{\partial f}{\partial y}\frac{\partial\theta}{\partial x}-\frac{\partial\theta}{\partial y}\frac{\partial f}{\partial x}\right)\tag{3.17}$$

Along with boundary conditions

$$\begin{aligned}&f=f'=0,\quad \theta=1 \qquad \text{at}\quad y=0\\ &f'\to 0,\quad \theta\to 0 \quad \text{as}\quad y\to\infty\end{aligned}\tag{3.18}$$

where primes denote differentiation of the function with respect to y.

It can be seen that near the lower stagnation point of the sphere, i.e., $x\approx 0$, Equations (3.16) and (3.17) reduce to the following ordinary differential equations:

$$f'''+2ff''-f'^2+\theta-Mf'=0\tag{3.19}$$

$$\frac{1}{Pr}\left[\left\{1+\frac{4}{3}Rd\left(1+(\theta_w-1)\theta\right)^3\right\}\theta'\right]'+2f\theta'+Q\theta=0\tag{3.20}$$

Subject to the boundary conditions

$$f(0) = f'(0) = 0, \quad \theta(0) = 1$$
$$f' \to 0, \quad \theta \to 0 \quad \text{as} \quad y \to \infty \tag{3.21}$$

In practical applications, the physical quantities of principle interest are the shearing stress τ_w, the rate heat transfer and the rate of species concentration transfer in terms of the skin-friction coefficients C_{fx} and Nusselt number Nu_x, which can be written in non-dimensional form as

$$Nu_x = \frac{aGr^{-1/4}}{k(T_w - T_\infty)} q_w \text{ and } \quad C_{fx} = \frac{Gr^{-3/4}a^2}{\mu\upsilon}\tau_w \tag{3.22}$$

where, $q_w = -k\left(\frac{\partial T}{\partial \hat{y}}\right)_{\hat{y}=0}$ and $\tau_w = \mu\left(\frac{\partial \hat{u}}{\partial \hat{y}}\right)_{\hat{y}=0}$, q_w is the heat flux at the surface and k being the thermal conductivity of the fluid.

Using the new variables (3.7), we have

$$q_w = -k\left(\frac{\partial(T_\infty + \theta(T_w - T_\infty))}{\partial(aGr^{-1/4}y}\right)_{y=0} = -\frac{k(T_w - T_\infty)}{aGr^{-1/4}}\left(\frac{\partial\theta}{\partial y}\right)_{y=0}$$

$$\text{and } \tau_w = \mu\left(\frac{\partial(\upsilon u Gr^{1/2}/a)}{\partial(aGr^{-1/4}y)}\right)_{y=0} = \frac{\mu\upsilon Gr^{1/2}}{a^2Gr^{-1/4}}\left(\frac{\partial u}{\partial y}\right)_{y=0} = \frac{\mu\upsilon}{a^2G_r^{-3/4}}\left(\frac{\partial u}{\partial y}\right)_{y=0}$$

Putting the above values in Equations (3.22), we have

$$Nu_x = \frac{aGr^{-1/4}}{k(T_w - T_\infty)} \times -\frac{k(T_w - T_\infty)}{aGr^{-1/4}}\left(\frac{\partial\theta}{\partial y}\right)_{y=0} = -\left(\frac{\partial\theta}{\partial y}\right)_{y=0}$$

$$\therefore Nu_x = -\left(\frac{\partial \theta}{\partial y}\right)_{y=0} \tag{3.23}$$

and $C_{fx} = \frac{Gr^{-3/4}a^2}{\mu\nu} \times \frac{\mu\nu}{a^2 Gr^{-3/4}} \left(\frac{\partial u}{\partial y}\right)_{y=0} = \left(\frac{\partial u}{\partial y}\right)_{y=0}$

$= x\left(\frac{\partial^2 f}{\partial y^2}\right)_{y=0}$, since $u = x\frac{\partial f}{\partial y}$

$$\therefore C_{fx} = x\left(\frac{\partial^2 f}{\partial y^2}\right)_{y=0} \tag{3.24}$$

We discuss velocity distribution as well as temperature profiles for a selection of parameter sets consisting of heat generation parameter, MHD parameter, and the Prandlt number at different position of x.

3.3 Results and discussion

In this context we have investigated analytically the effect of radiation on magnetohydrodynamic natural convection flow on a sphere in presence of heat generation. Solutions are obtained for fluids having Prandtl number Pr = 0.72 (air) and for some values of Pr = 1.00, 1.74 and 2.50 against y for a wide range of values of radiation parameter Rd, surface temperature parameter θ_w, heat generation parameter Q and magnetic parameter M. We have considered the values of heat generation parameter Q = 0.2, 0.3, 0.5 and 0.6 with radiation parameter Rd=1.0, Prandtl number Pr = 0.72 and surface temperature parameter θ_w = 1.1 and magnetic parameter M=0.1. The values of radiation parameter Rd =1.0, 1.2, 1.5 and 2.0 have been taken in case of Q = 0.2, Pr = 0.72, θ_w = 1.1 and magnetic parameter M=0.1. The different values of surface temperature parameter θ_w = 0.4, 1.1, 1.4 and 1.6 are considered with Q = 0.2, Pr = 0.72 and Rd =1.0and M=0.1. Different values of magnetic parameter M=0.1. 0.3, 0.5 and 0.7 have been taken in case of Q = 0.2, Pr = 0.72, θ_w = 1.1 and Rd =1.0. Numerical values of local rate of heat transfer are calculated in terms of Nusselt number Nu for the surface of the sphere from lower stagnation point to upper

stagnation point. The effect for different values of heat generation parameter Q and magnetic parameter M on local skin friction coefficient C_f and the local Nusselt number Nu, as well as velocity and temperature profiles with the Prandtl number $Pr = 0.72$, radiation parameter Rd =1.0 and surface temperature parameter $\theta_w = 1.1$, are also observed.

Figures 3.1-3.2 display results for the velocity and temperature profiles, for different values of heat generation parameter Q while Prandtl number $Pr = 0.72$, radiation parameter Rd =1.0 surface temperature parameter $\theta_w = 1.1$ and magnetic parameter M=0.1. It has been seen from Figures 3.1 and 3.2 that as the heat generation parameter Q increases, the velocity and the temperature profiles increase. The changes of velocity profiles in the y direction reveals the typical velocity profile for natural convection boundary layer flow, i.e., the velocity is zero at the boundary wall then the velocity increases to the peak value as y increases and finally the velocity approaches to zero (the asymptotic value). The changes of temperature profiles in the y direction also shows the typical temperature profiles for natural convection boundary layer flow that is the value of temperature profiles is 1.0 (one) at the boundary wall then the temperature profile decreases gradually along y direction to the asymptotic value.

The variation of the velocity and temperature profiles for different values of radiation parameter Rd in case of surface temperature parameter $\theta_w = 1.1$, Prandtl number $Pr = 0.72$, heat generation parameter $Q = 0.2$ and magnetic parameter M=0.1 are shown in Figures 3.3 and 3.4. Here, as the radiation parameter Rd increases, both the velocity and the temperature profiles increase slightly such that there exists a local maximum of the velocity within the boundary layer, but velocity increases near the surface of the sphere and then temperature decreases slowly and finally approaches to zero.

The effect for different values of surface temperature parameterθ_w, the velocity and temperature profiles with Prandtl number $Pr = 0.72$, heat generation parameter $Q = 0.2$, radiation parameter Rd =1.0 and magnetic parameter M=0.1 are shown in Figures 3.5 and 3.6. Here, as the surface temperature parameter θ_w increases, the velocity and the temperature profiles increase slightly such that there exists a local maximum of the velocity within the boundary layer, but velocity increases near the surface of the sphere and then temperature decreases slowly and finally approaches to zero. However, in Figures 3.7 and 3.8. It has been shown that when the Prandtl number $Pr = 0.72$, 1.00, 1.74 and 2.50 increases

with θ_w = 1.1, Rd =1.0, Q = 0.5 and M=0.1, both the velocity and temperature profiles decrease.

Figures 3.9 display results for the velocity profiles for different values of magnetic parameter M with Prandtl number Pr = 0.72, radiation parameter Rd =1.0, heat generation parameter Q = 0.2 and surface temperature parameter θ_w = 1.1. It has been seen from Figure 3.9 that as the magnetic parameter M increases, the velocity profiles decrease upto the position of y = 3.34 after that position velocity profiles increase with the increase of magnetic parameter. It is also observed from Figure 3.9 that the changes of velocity profiles in the y direction reveals the typical velocity profile for natural convection boundary layer flow, i.e., the velocity is zero at the boundary wall then the velocity increases to the peak value as y increases and finally the velocity approaches to zero (the asymptotic value) but we see from this figure and its magnified portion all the velocity profiles meet together at the position of y = 3.34 and cross the side. This is because of the velocity profiles having lower peak values for higher values of magnetic parameter tend to decrease comparatively slower along y direction than velocity profiles with higher peak values for lower values of magnetic parameter. Figure 3.10 display results for the temperature profiles, for different values of magnetic parameter M while Prandtl number Pr = 0.72, radiation parameter Rd =1.0, heat generation parameter Q = 0.2 and surface temperature parameter θ_w = 1.1. The maximum values of velocity are recorded to be 0.46181, 0.43333, 0.40700 and 0.38293 for M=0.1, 0.3, 0.5 and 0.7 respectively which occur at the same point y = 1.23788. Here, it is observed that at y = 1.23788, the velocity decreases by 20.077% as the magnetic parameter M changes from 0.1 to 0.7. The changes of temperature profiles in the y direction also shows the typical velocity profile for natural convection boundary layer flow that is the value of temperature profile is 1.0 (one) at the bonndary wall then the temperature profile decreases gradually along y direction to the asymptotic value.

From Figure 3.11 we observed that the skin friction coefficient C_f increases significantly as the heat generation parameter Q increases. This means that for increasing the heat generation effect, the fluid temperature also increases. In this case surface temperature is less than fluid temperature and that is the skin friction coefficient increases. Figure 3.12 show that heat transfer coefficient Nu decreases for increasing values of heat generation parameter Q with

Prandtl number Pr = 0.72, radiation parameter Rd =1.0, surface temperature parameter θ_w = 1.1 and magnetic parameter M=0.1. It is observed from Figure 3.11 that the skin friction increases gradually from zero value at lower stagnation point along the x direction and from Figure 3.12, it reveals that the rate of heat transfer decreases along the x direction from lower stagnation point to the downstream.

The effect for different values of radiation parameter Rd, the skin friction coefficient and heat transfer coefficient while Prandtl number Pr = 0.72, heat generation parameter Q = 0.2, surface temperature parameter θ_w = 1.1 and magnetic parameter M=0.1 are shown in Figures 3.13- 3.14. Here, as the radiation parameter Rd increases, both the skin friction coefficient and heat transfer coefficient increase.

From Figures 3.15 - 3.16, it can also easily be seen that an increase in the surface temperature parameter θ_w leads to increase in the local skin friction coefficient C_f and the local rate of heat transfer Nu slightly while Prandtl number Pr = 0.72, heat generation parameter Q = 0.2, radiation parameter Rd =1.0 and magnetic parameter M=0.1. It is also observed that at any position of x, the skin friction coefficient C_f and the local Nusselt number Nu increase as θ_w increases from 0.8 to 1.6. This phenomenon can easily be understood from the fact that when the surface temperature parameter θ_w increases, the temperature of the fluid rises and the thickness of the velocity boundary layer grows, i.e., the thermal boundary layer becomes thinner than the velocity boundary layer. Therefore the skin friction coefficient C_f and the local Nusselt number Nu increases.

The variation of the local skin friction coefficient C_f and local rate of heat transfer Nu for different values of Prandtl number Pr while θ_w = 1.1, Rd =1.0, Q = 0.2 and M=0.1 are shown in Figures 3.17 and 3.18. We can observe from these figures that as the Prandtl number Pr increases, the skin friction coefficient decreases and rate of heat transfer increases but the rate of increase in the heat transfer coefficient is higher than that of the skin friction coefficient so, the effect of Prandtl number Pr on heat transfer coefficient is more than the at of the effect of Pr on skin friction coefficient.

Figures 3.19-3.20 show that skin friction coefficient C_f and heat transfer coefficient Nu decrease for increasing values of magnetic parameter M while heat generation parameter

Q=0.2,.Prandtl number Pr = 0.72, radiation parameter Rd =1.0 and surface temperature parameter θ_w = 1.1. The values of skin friction coefficient C_f and Nusselt number Nu are recorded to be 1.06755, 0.99745, 0.93565, 0.88141 and 0.44468, 0.40643, 0.36999, 0.33515 for M=0.1. 0.3, 0.5 0.7 respectively which occur at the same point x = 1.57080. Here, it observed that at x = 1.57080, the skin friction decreases by 17.437% and Nusselt number Nu decreases by 24.631% as the magnetic parameter M changes from 0.1 to 0.7. It is observed from Figure 3.19 that the skin friction decreases gradually from zero value at lower stagnation point along the x direction and from Figure 3.20, it reveals that the rate of heat transfer decreases along the x direction from lower stagnation point to the downstream.

Numerical values of rate of heat transfer Nu and skin friction coefficient C_f are calculated from Equations (3.23) and (3.24) for the surface of the sphere from lower stagnation point at x = 0^0 to x = 90^0. Numerical values of C_f and Nu are shown in Table 3.1.

Table 3. 1: Skin friction coefficient and rate of heat transfer against x for different values of magnetic parameter M with other controlling parameters Pr = 0.72, Rd = 1.0, θ_w =1.1.and Q = 0.2.

	M= 0.1		M= 0.3		M= 0.5		M= 0.7	
x	C_f	Nu	C_f	Nu	C_f	Nu	C_f	Nu
0.00000	0.00000	0.64019	0.00000	0.60741	0.00000	0.57605	0.00000	0.54594
0.10472	0.09349	0.63929	0.08872	0.60647	0.08441	0.57510	0.08055	0.54498
0.20944	0.18633	0.63676	0.17679	0.60387	0.16819	0.57244	0.16047	0.54225
0.31416	0.27792	0.63259	0.26362	0.59958	0.25073	0.56803	0.23915	0.53774
0.40143	0.35285	0.62785	0.33458	0.59470	0.31812	0.56303	0.30335	0.53262
0.50615	0.44055	0.62063	0.41752	0.58728	0.39680	0.55541	0.37822	0.52483
0.61087	0.52528	0.61172	0.49751	0.57812	0.47254	0.54602	0.45017	0.51521
0.71558	0.60646	0.60110	0.57395	0.56719	0.54476	0.53481	0.51864	0.50374
0.80285	0.67098	0.59092	0.63454	0.55672	0.60185	0.52406	0.57263	0.49274
0.90757	0.74418	0.57707	0.70303	0.54247	0.66617	0.50945	0.63329	0.47778
1.01229	0.81224	0.56140	0.76640	0.52635	0.72542	0.49291	0.68893	0.46086
1.20428	0.92196	0.52777	0.86762	0.49178	0.81922	0.45745	0.77630	0.42458
1.57080	1.06755	0.44468	0.99745	0.40643	0.93565	0.36999	0.88141	0.33515

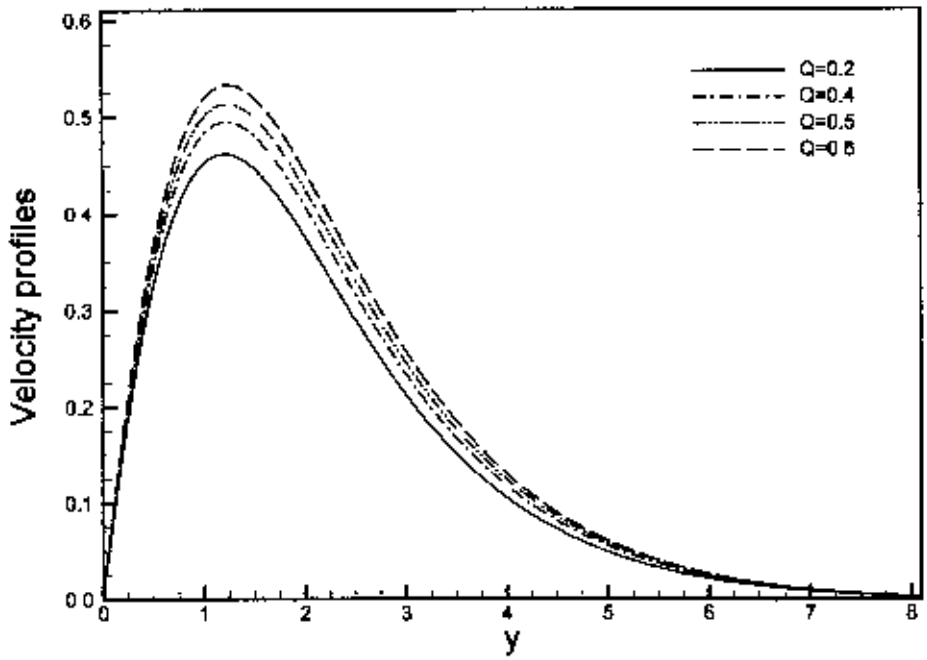

Figure 3.1: Velocity profiles for different values of Q in case of $Pr = 0.72$, $Rd = 1.0$, $\theta_w = 1.1$ and $M = 0.1$

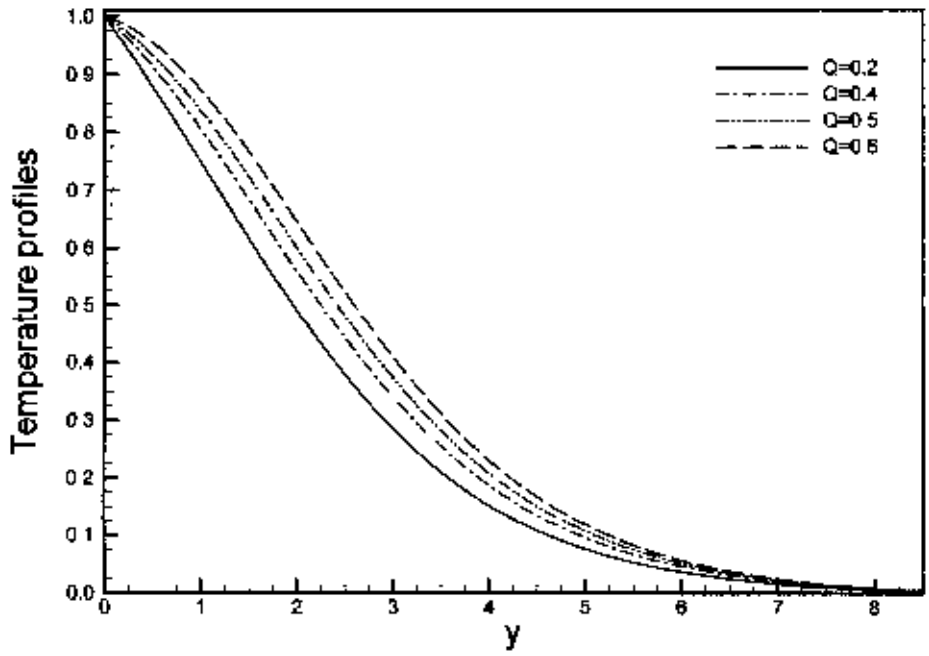

Figure 3.2: Temperature profiles for different values of Q in case of $Pr = 0.72$, $Rd = 1.0$, $\theta_w = 1.1$ and $M = 0.1$

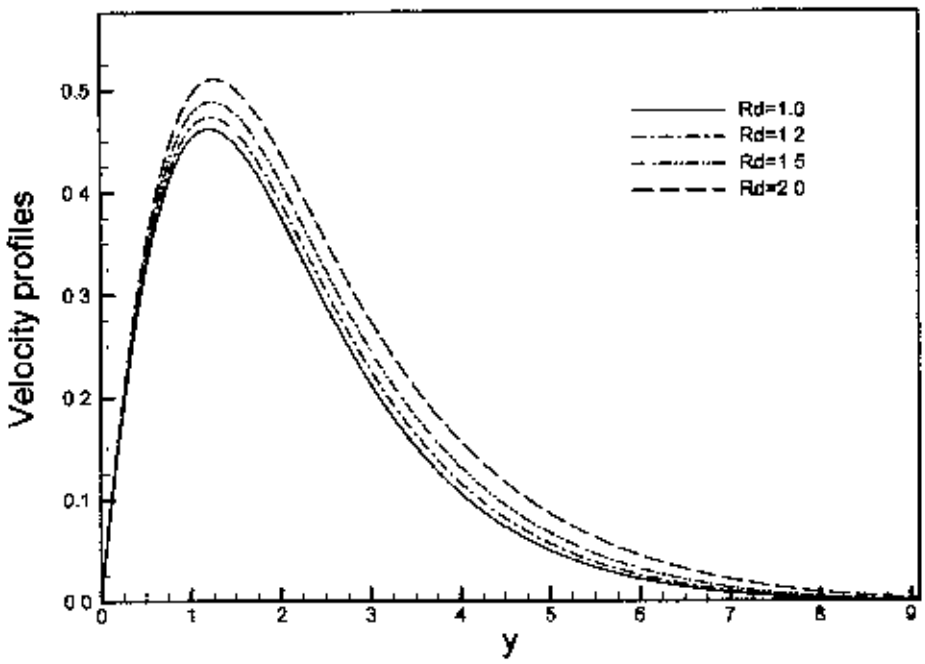

Figure 3.3: Velocity profiles for different values of *Rd* in case of $Pr = 0.72$, $\theta_w = 1.1$, Q=0.2 and $M = 0.1$

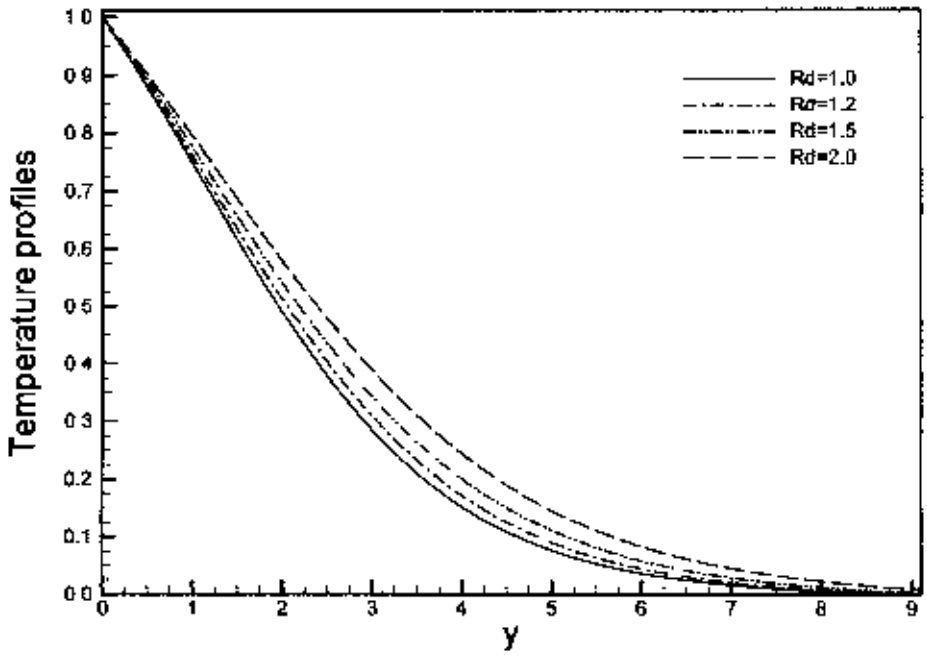

Figure 3.4: Temperature profiles for different values *Rd* in case of $Pr = 0.72$, $\theta_w = 1.1$, $Q=0.2$ and $M = 0.1$

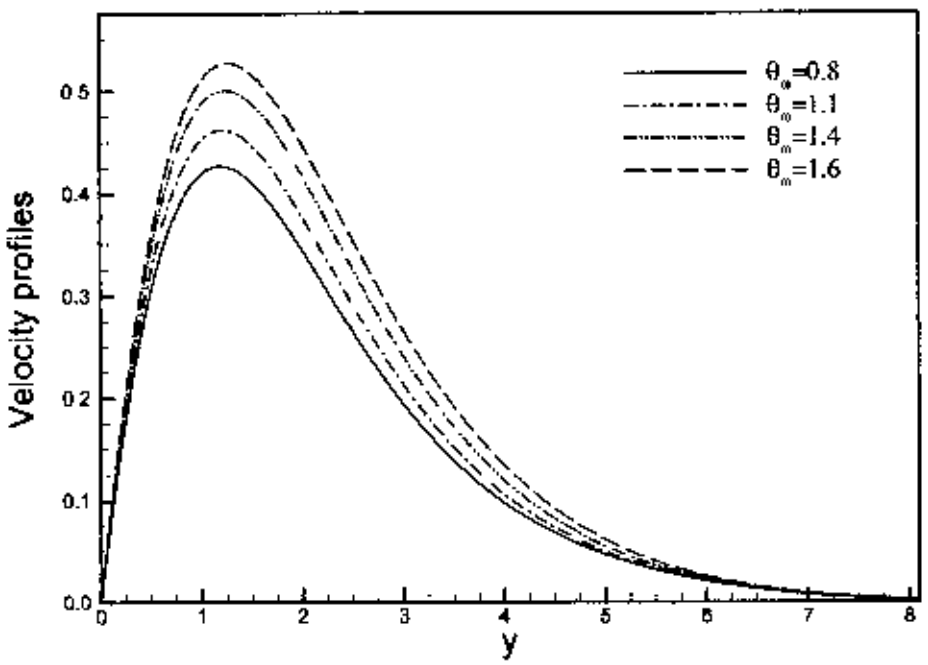

Figure 3.5: Velocity profiles for different values of θ_w in case of $Pr = 0.72$, $Rd = 1.0$, $Q = 0.2$ and $M = 0.1$

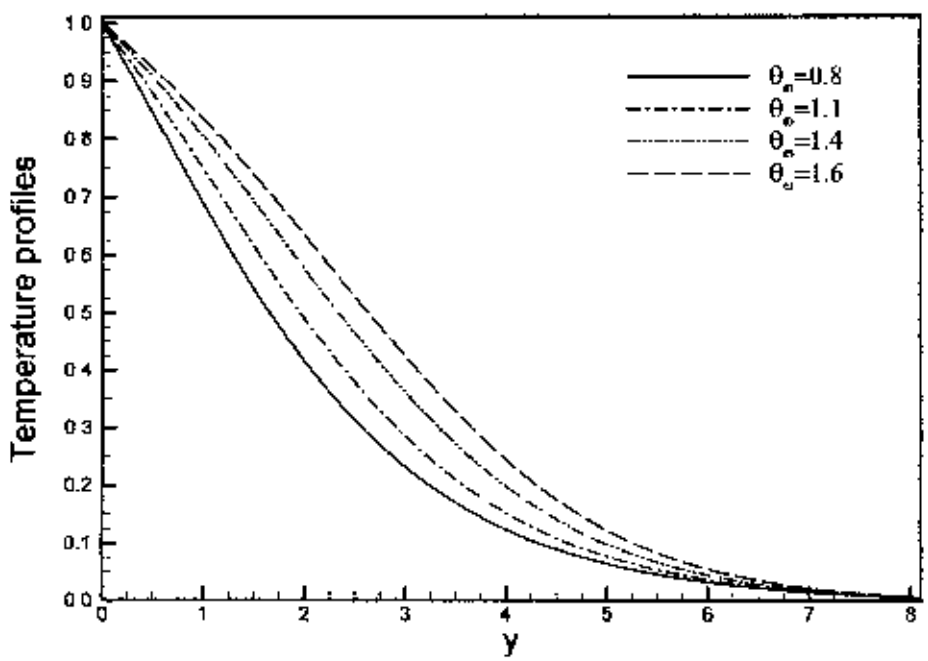

Figure 3.6: Temperature profiles for different values of θ_w in case of $Pr = 0.72$, $Rd = 1.0$, $Q = 0.2$ and $M = 0.1$

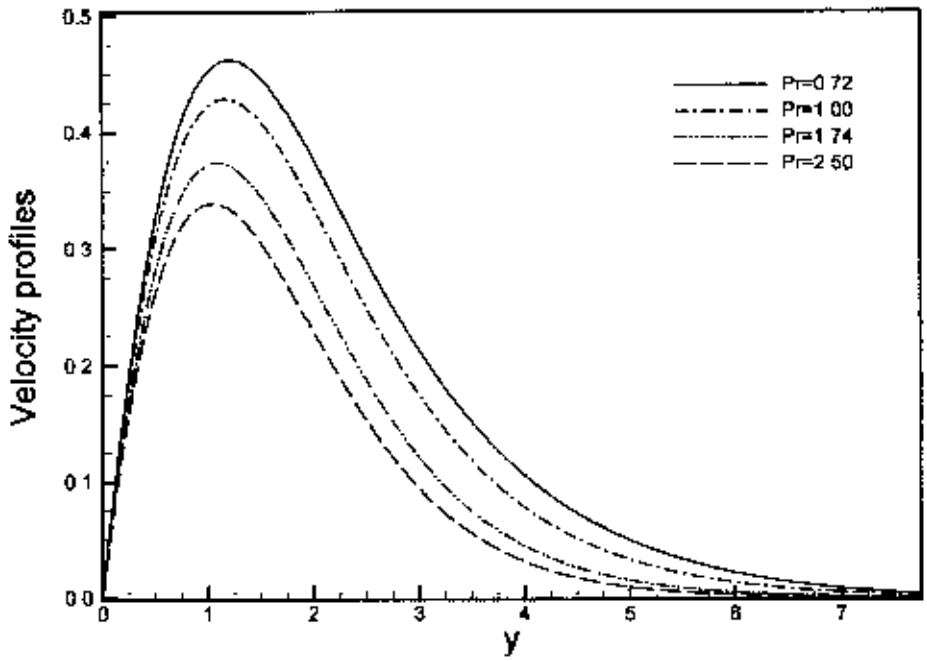

Figure 3.7: Velocity profiles for different values of Pr in case of Rd =1.0, θ_w =1.1 , Q=0.2 and M= 0.1

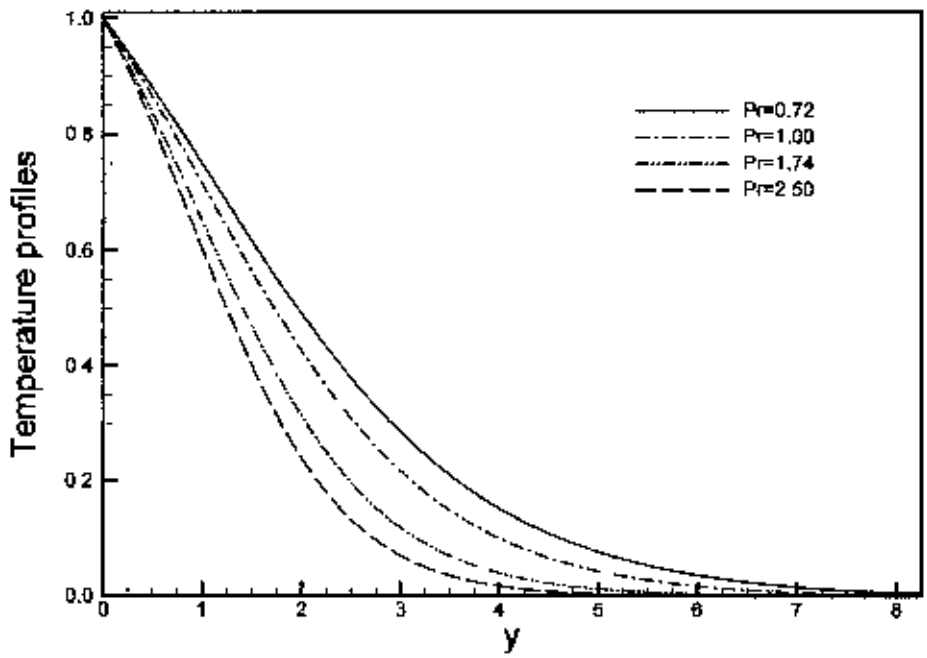

Figure 3.8: Temperature profiles for different values of Pr in case of Rd =1.0, θ_w =1.1 , Q=0.2 and M= 0.1

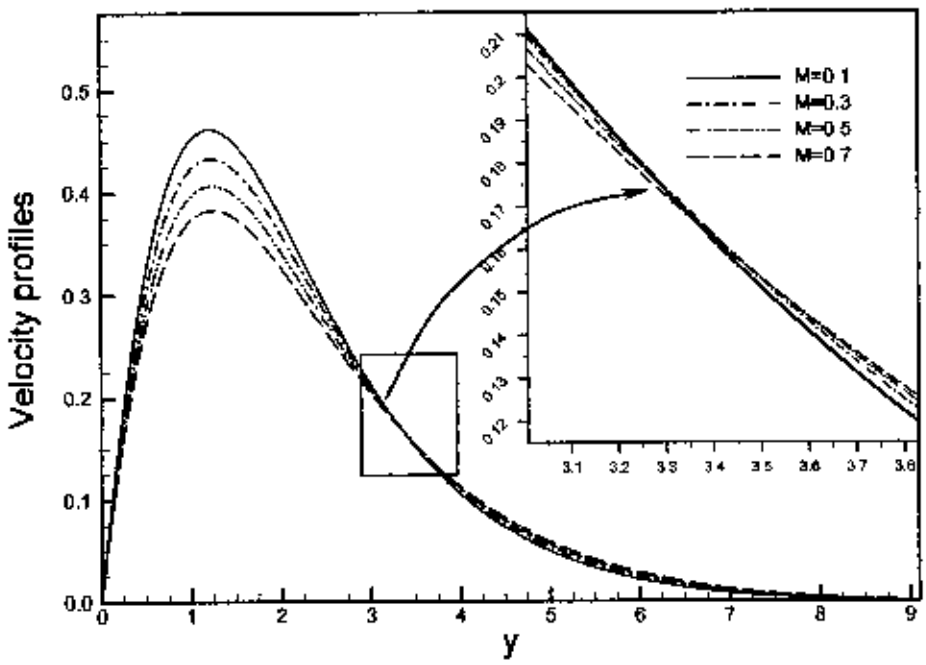

Figure 3.9: Velocity profiles for different values of M in case of Rd =1.0, θ_w =1.1, Q=0.2 and Pr=0.72

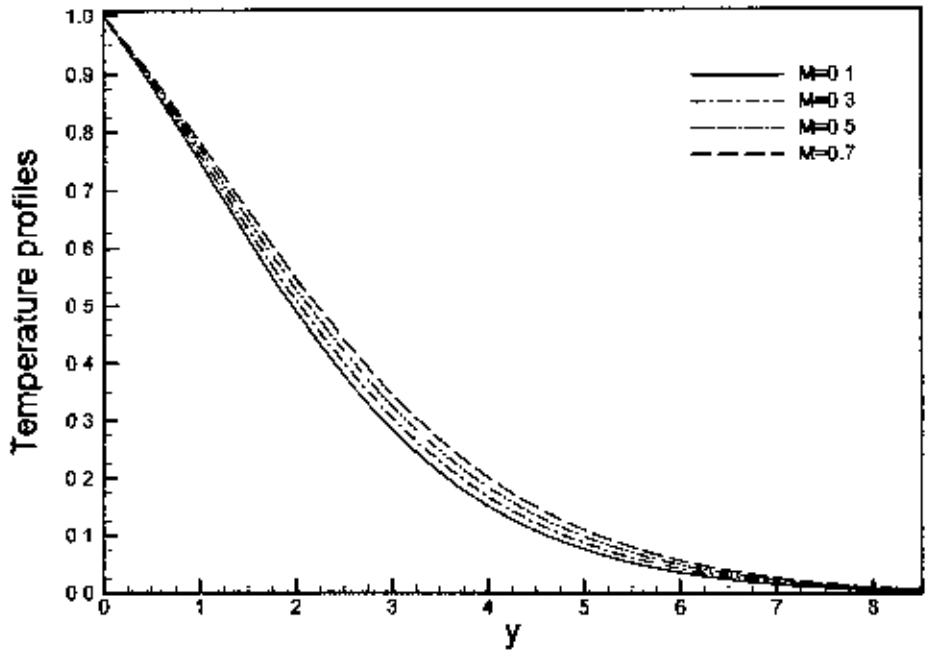

Figure 3.10: Temperature profiles for different values of M in case of Rd =1.0, θ_w =1.1, Q=0.2 and Pr=0.72

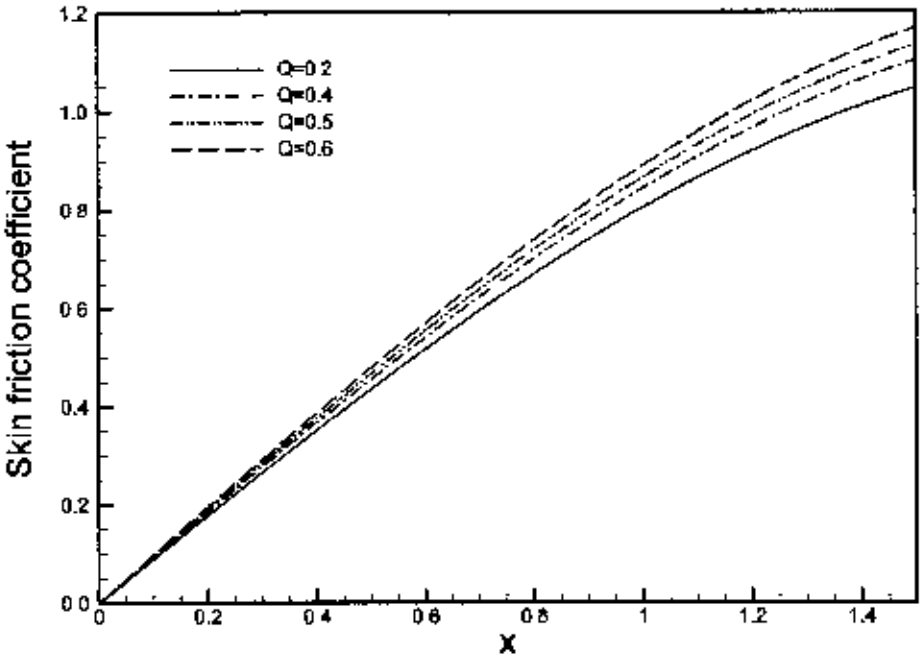

Figure 3.11: Skin-friction coefficient for different values of Q in case of $Pr = 0.72$, $Rd = 1.0$, $\theta_w = 1.1$ and $M = 0.1$

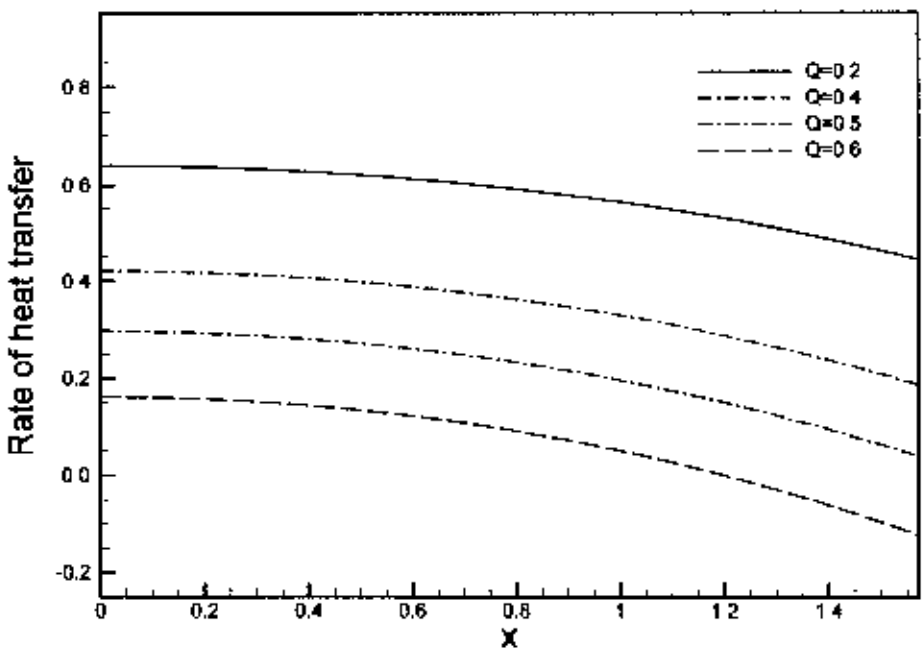

Figure 3.12: Rate of heat transfer for different values of Q in case of $Pr = 0.72$, $Rd = 1.0$, $\theta_w = 1.1$ and $M = 0.1$

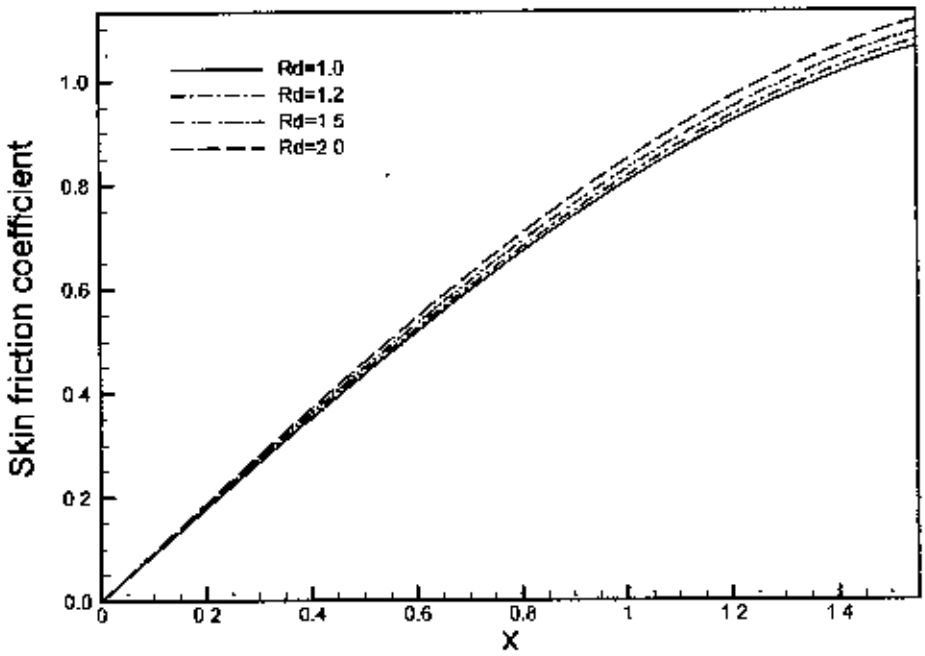

Figure 2.13: Skin-friction coefficient for different values of Rd in case of $Pr = 0.72$, $\theta_w = 1.1$, $Q = 0.2$ and $M = 0.1$

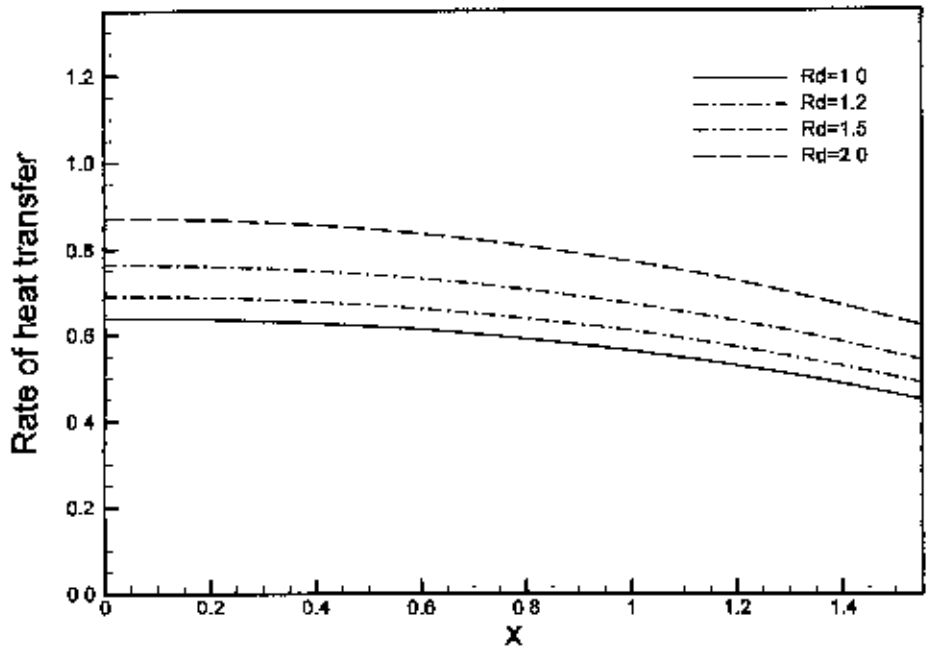

Figure 3.14: Rate of heat transfer for different values of Rd in case of $Pr = 0.72$, $\theta_w = 1.1$, $Q = 0.2$ and $M = 0.1$

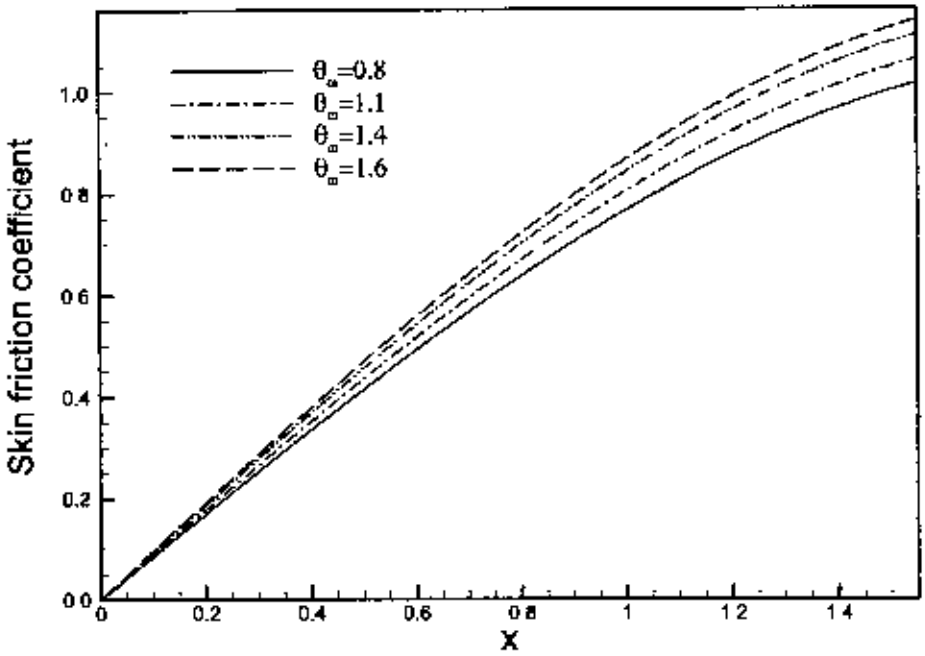

Figure 3.15: Skin-friction coefficient for different values of θ_w in case of $Pr = 0.72$, $Rd = 1.0$, $Q = 0.2$ and $M = 0.1$

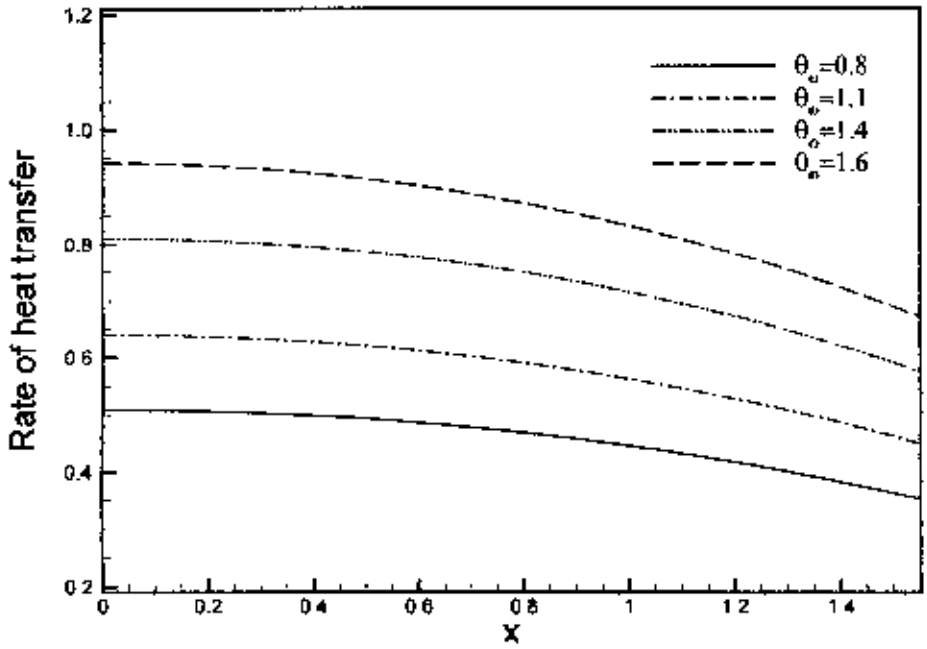

Figure 3.16: Rate of heat transfer for different values of θ_w in case of $Pr = 0.72$, $Rd = 1.0$, $Q = 0.2$ and $M = 0.1$

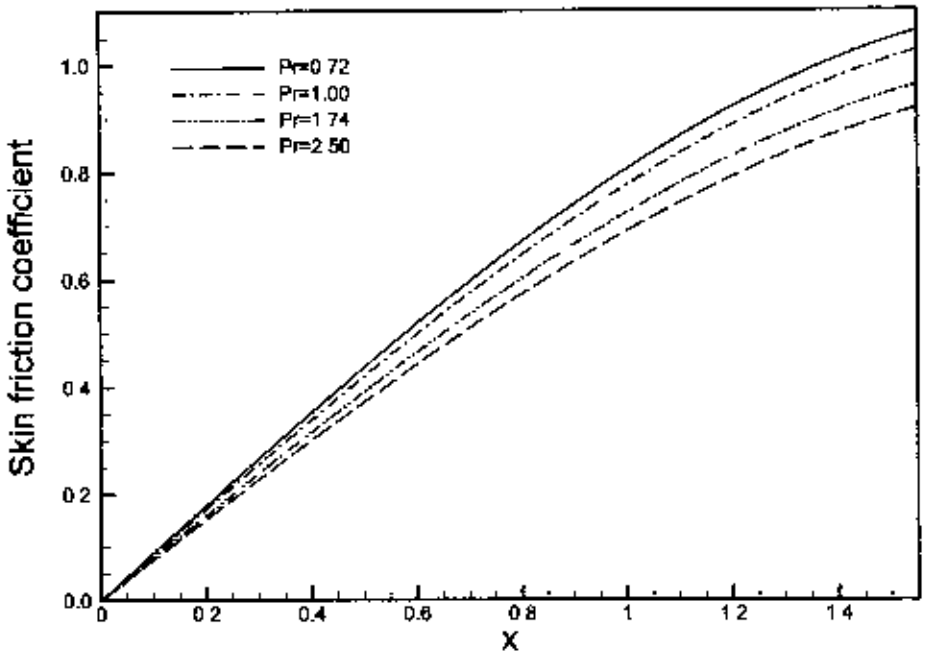

Figure 3.17: Skin-friction coefficient for different values of Pr in case of Rd =1.0, θ_w =1.1, Q=0.2 and M= 0.1

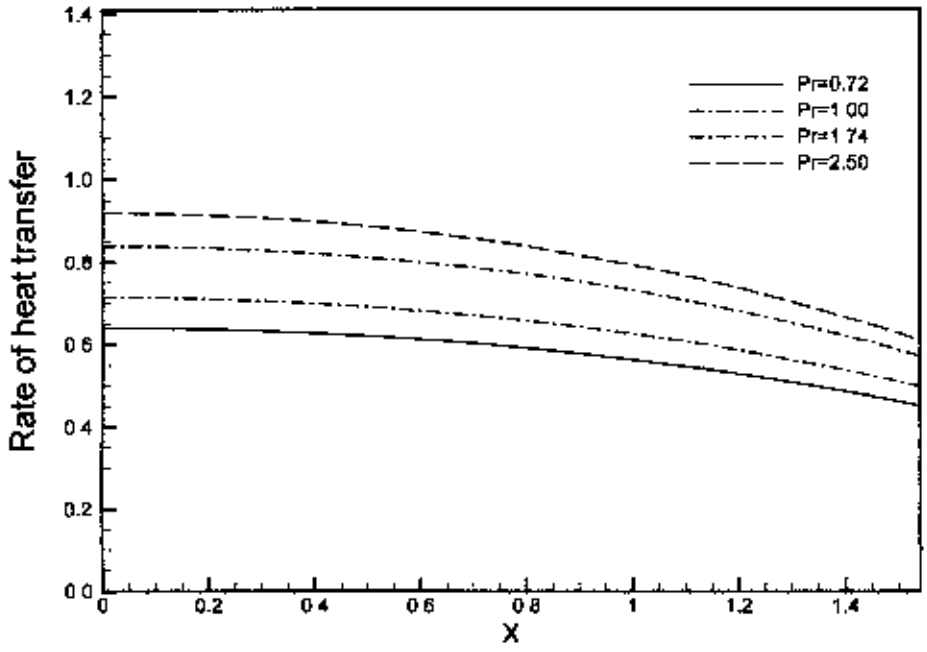

Figure 3.18: Rate of heat transfer for different values of Pr in case of Rd =1.0, θ_w =1.1, Q=0.2 and M= 0.1

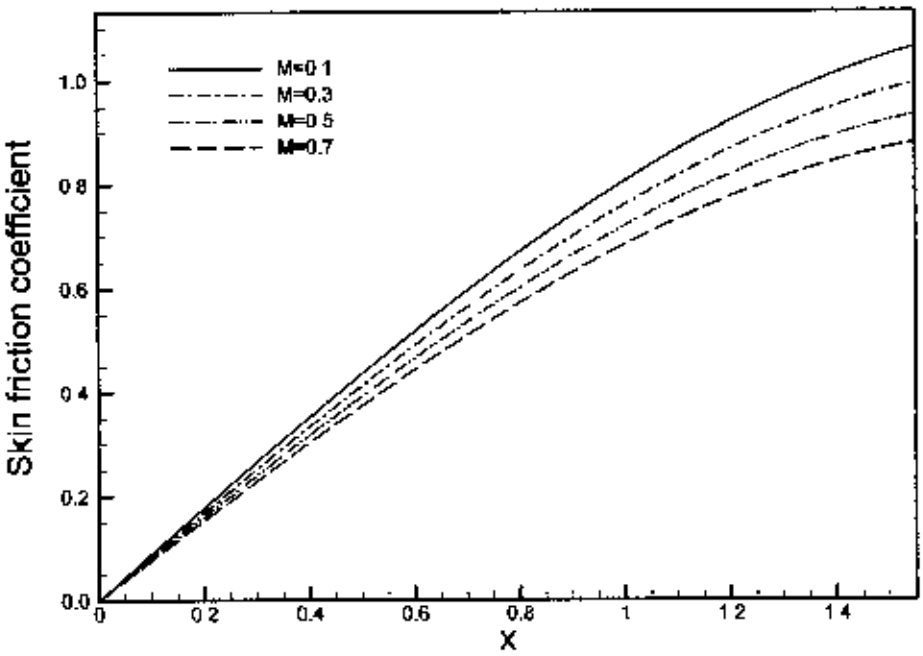

Figure 3.19: Skin-friction coefficient for different values of M in case of $Pr = 0.72$, Rd =1.0, θ_w =1.1 and Q=0.2

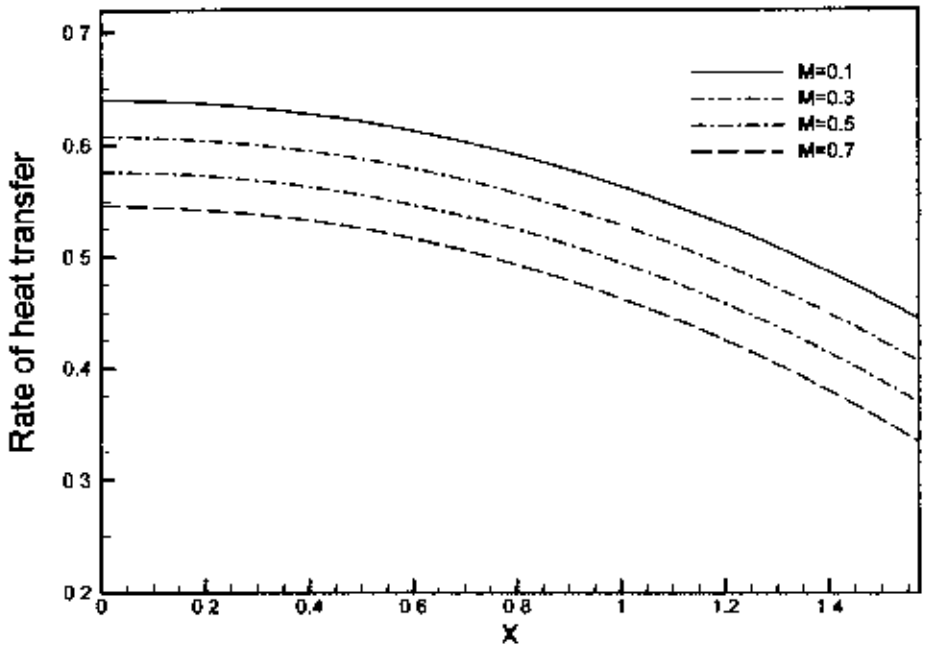

Figure 3.20: Rate of heat transfer for different values of M in case of $Pr = 0.72$, Rd =1.0, θ_w =1.1 and Q=0.2

3.4 Comparison of the results

Figure 3.21 depicts the comparisons of the present numerical results of the Nusselt number Nu with those obtained by Nazar et al. (2002) and Huang and Chen (1987). Here, the radiation, heat generation and magnetic effects are ignored (i.e., Rd =0.0, Q=0.0 and M =0.0) and Prandtl numbers Pr = 0 7 and 7.0 are chosen. I studied well the results and it helped me to take firm decision that the present results agreed well with the solutions of Nazar et al. (2002) and Huang and Chen (1987) in the absence of suction and blowing

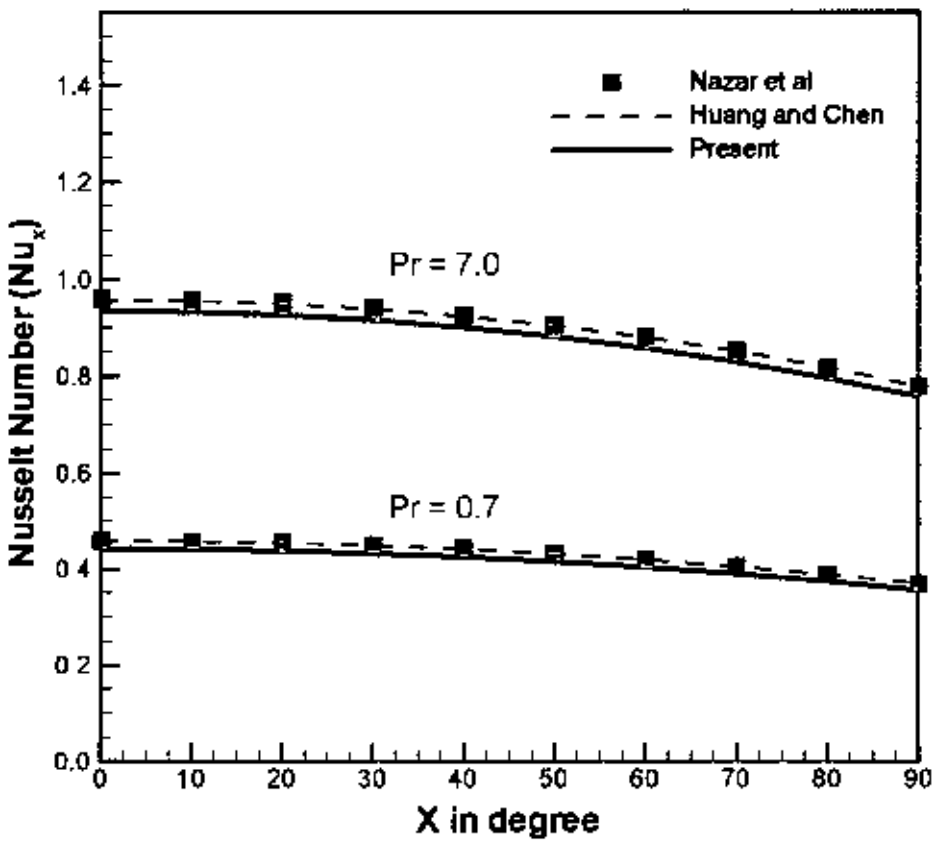

Figure 3.21: Comparisons of the present numerical results of Nusselt number Nu for the Prandtl numbers Pr = 0.7, 7.0 with those obtained by Nazar et al. (2002) and Huang and Chen (1987).

Figure 3 22 shows the comparisons of the present numerical results of the skin friction coefficients C_{fx} with those obtained by Taher and Molla (2005) for different values of heat generation parameter which are Q = 2.0, 1.5 and 1.0. Here, the radiation and the magnetic effects are ignored (i.e , Rd =0.0 and M =0.0) and Prandtl numbers Pr = 0.7 have been chosen. The comparison shows fairly good agreement between the present results and the results of Taher and Molla (2005).

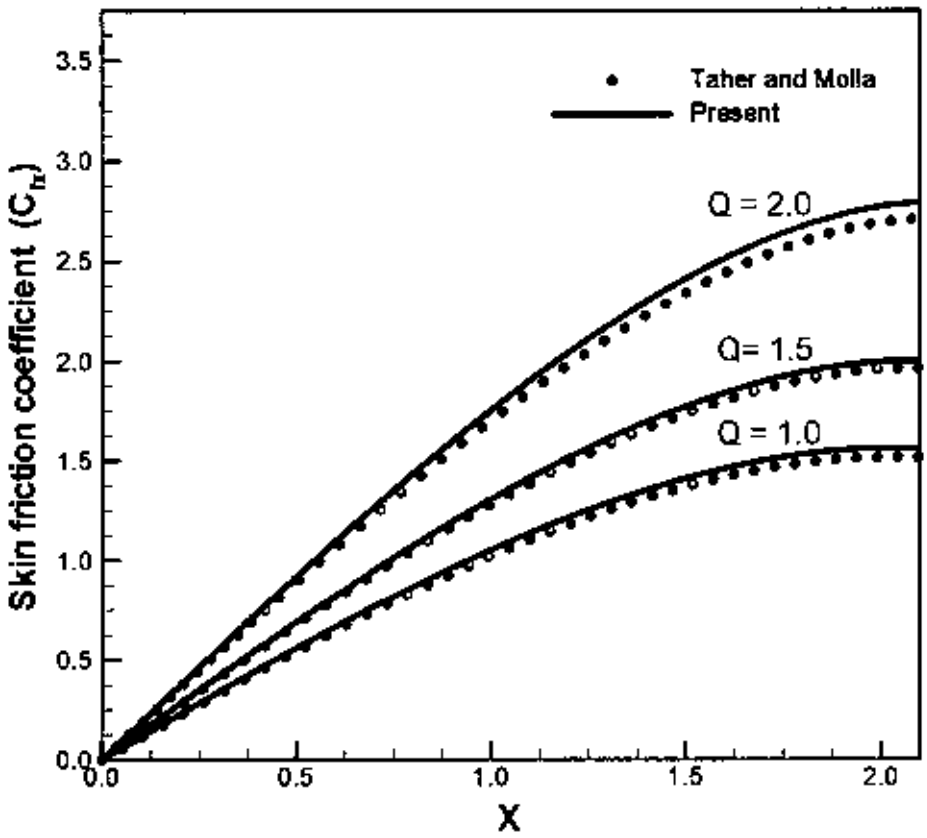

Figure 3.22: Comparisons of the present numerical results of Skin friction coefficient C_{fx} for the heat generation parameter Q = 2.0, 1.5 and 1.0 with those obtained by Taher and Molla (2005).

3.5 Conclusion

The effect of radiation on natural convection flow on a sphere in presence of heat generation has been investigated for different values of relevant physical parameters including the magnetic parameter M. The governing boundary layer equations of motion are transformed into a non-dimensional form and the resulting non-linear systems of partial differential equations are reduced to local non-similarity boundary layer equations, which are solved numerically by using implicit finite difference method together with the Keller-box scheme. From the present investigation the following conclusions may be drawn:

- Significant effects of heat generation parameter Q and magnetic parameter M on velocity and temperature profiles as well as on skin friction coefficient C_f and the rate of heat transfer Nu have been found in this investigation but the effect of heat generation parameter Q and magnetic parameter M on rate of heat transfer is more significant. An increase in the values of heat generation parameter Q leads to both the velocity and the temperature profiles increase, the local skin friction coefficient C_f increases at different position of y but the local rate of heat transfer Nu decreases at different position of x for Pr =0.72.

- All the velocity profile, temperature profile, the local skin friction coefficient C_f and the local rate of heat transfer Nu increase significantly when the values of radiation parameter Rd increases.

- As surface temperature parameter θ_w increases, both the velocity and the temperature profile increase and also the local skin friction coefficient C_f and the local rate of heat transfer Nu increase significantly.

- For increasing values of Prandtl number Pr leads to decrease the velocity profile, the temperature profile and the local skin friction coefficient C_f but the local rate of heat transfer Nu increases.

- An increase in the values of M leads to decrease the velocity profiles but to increase the temperature profiles and also both the local skin friction coefficient C_f and the local rate of heat transfer Nu decrease.

3.6 Extension of this work

In this work, we considered constant viscosity and thermal conductivity but they are functions of temperature.

- If we consider the viscosity and thermal conductivity as the function of temperature then we can extend our problem.
- Also taking the non-uniform surface temperature, the problem can be extended.

Appendix

Implicit Finite Difference Method

To get the solutions of the transformed governing equations with the corresponding boundary conditions, we employed implicit finite difference method together with Keller-box elimination technique which is well documented and widely used by Keller and Cebeci (1971) and recently by Hossain et al. (1990, 1992, 1996. 1997, 1998).

A brief discussion on the development of algorithm on the method of implicit finite difference method together with Keller – box elimination scheme is given below considering the following Equations (A1-A2).

$$f''' + \left(1 + \frac{x}{\sin x}\cos x\right) ff'' - (f')^2 + \frac{\sin x}{x}\theta - Mf' = x\left(f'\frac{\partial f'}{\partial x} - \frac{\partial f}{\partial x}f''\right) \tag{A1}$$

and

$$\frac{1}{pr}\theta'' + \left(1 + \frac{x}{\sin x}\cos x\right) f\theta' = x\left(f'\frac{\partial \theta}{\partial x} - \frac{\partial f}{\partial x}\theta'\right) \tag{A2}$$

To apply the aforementioned method, we first convert Equations (A1)-(A2) into the following system of first order equations with dependent variables $u\ (\xi, \eta)$, $v\ (\xi, \eta)$, $p\ (\xi, \eta)$, and $g\ (\xi, \eta)$ as

$$f' = u\ ,\ u' = v,\quad g = \theta,\ \text{and}\ \ \theta' = p \tag{A3}$$

$$v' + p_1 fv - p_2 u^2 + p_3 g - p_4 u = \xi\left(u\frac{\partial u}{\partial \xi} - \frac{\partial f}{\partial \xi}v\right) \tag{A4}$$

$$\frac{1}{\Pr}p' + p_1 fp = \xi\left(u\frac{\partial g}{\partial \xi} - p\frac{\partial f}{\partial \xi}\right) \tag{A5}$$

where

$$x = \xi\ ,\ p_1 = 1 + \frac{x}{\sin x}\cos x\ ,\ p_2 = 1,\ p_3 = \frac{\sin x}{x}\ ,\ p_4 = M \tag{A6}$$

The corresponding boundary conditions are

$$f(\xi, 0) = 0,\ u(\xi, 0) = 0 \text{ and } g(\xi, 0) = 0$$
$$u(\xi, \infty) = 0,\ g(\xi, \infty) = 0 \tag{A7}$$

We now consider the net rectangle on the (ξ, η) plane and denote the net point by

$$\eta_0 = 0, \quad \eta_j = \eta_{j-1} + h_j, \quad j = 1, 2, \ldots J$$
$$\xi^0 = 0, \quad \xi^n = \xi^{n-1} + k_n, \quad n = 1, 2, \ldots N \tag{A8}$$

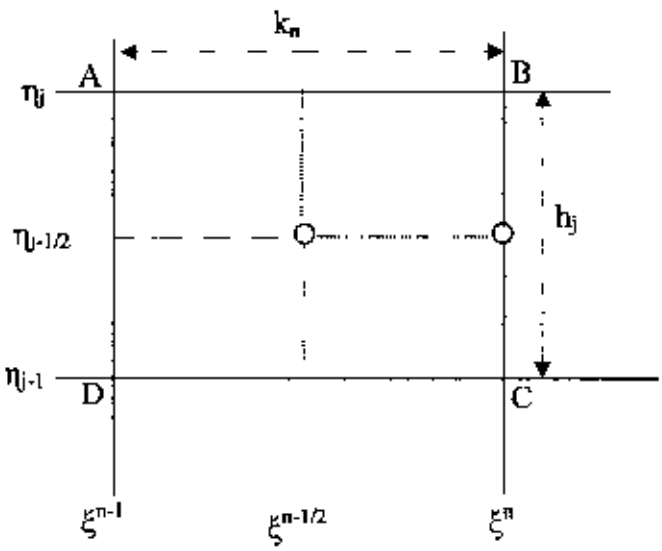

Figure A1: Net rectangle for difference approximations for the Box scheme

Here 'n' and 'j' are just sequence of numbers on the (ξ , η) plane , k_n and h_j are the variable mesh widths.

We approximate the quantities (f, u, v, p) at the points (ξ^n , η_j) of the net by (f^n_j , u^n_j , v^n_j ,p^n_j) which we call net function . We also employ the notation g^n_j for the quantities midway between net points shown in Figure (A1) and for any net function as

$$\xi^{n-1/2} = \frac{1}{2}(\xi^n + \xi^{n-1}) \tag{A9}$$

$$\eta_{j-1/2} = \frac{1}{2}(\eta_j - \eta_{j-1}) \tag{A10}$$

$$g_j^{n-1/2} = \frac{1}{2}(g_j^n + g_j^{n-1}) \tag{A11}$$

$$g^n_{j-1/2} = \frac{1}{2}(g_j^n + g^n_{j-1}) \tag{A12}$$

Now we write the difference equations that are to approximate Equations (A3) - (A4) by considering one mesh rectangle for the mid point (ξ^n, $\eta_{j-1/2}$) to obtain

$$\frac{f_j^n - f^n_{j-1}}{h_j} = u^n_{j-1/2} \tag{A13}$$

$$\frac{u_j^n - u^n_{j-1}}{h_j} = v^n_{j-1/2} \tag{A14}$$

$$\frac{g_j^n - g^n_{j-1}}{h_j} = p^n_{j-1/2} \tag{A15}$$

Similarly Equations (A5) –(A6) are approximate by centering about the mid point ($\xi^{n-1/2}$, $\eta_{j-1/2}$) . Centering the Equations (A9) about the point ($\xi^{n-1/2}$, η) without specifying η to obtain the algebraic equations. The difference approximation to Equations (A5)-(A6) become

$$\frac{1}{2}\left(L^n + L^{n-1}\right) = \xi^{n-\frac{1}{2}}\left[u^{n-\frac{1}{2}}\left(\frac{u^n - u^{n-1}}{k_n}\right) - v^{n-\frac{1}{2}}\left(\frac{f^n - f^{n-1}}{k_n}\right)\right] \tag{A16}$$

$$\frac{1}{2}\left(M^n + M^{n-1}\right) = \xi^{n-\frac{1}{2}}\left[u^{n-\frac{1}{2}}\left(\frac{g^n - g^{n-1}}{k_n}\right) - p^{n-\frac{1}{2}}\left(\frac{f^n - f^{n-1}}{k_n}\right)\right] \tag{A17}$$

Where

$$L^n = \left[v' + p_1 fv - p_2 u^2 + p_3 g - p_4 u\right]^n$$

$$L^{n-1} = \left[v' + p_1 fv - p_2 u^2 + p_3 g - p_4 u\right]^{n-1}$$

and

$$M^n = \left[\frac{1}{\mathrm{Pr}} p' + p_1 fp\right]^n$$

$$M^{n-1} = \left[\frac{1}{\mathrm{Pr}} p' + p_1 fp\right]^{n-1}$$

$$\left(v'\right)^n + \alpha_1\left(fv\right)^n - \alpha_2\left(u^2\right)^n + \alpha\left(v^{n-1} f^n - v^n f^{n-1}\right) + p_3 g^n - p_4 u^n = R^{n-1} \tag{A18}$$

$$\frac{1}{\mathrm{Pr}}\left(v'\right)^n + \alpha_1\left(fp\right)^n - \alpha\left(u^{n-1} g^n - u^n g^{n-1} + f^{n-1} p^n - f^n p^{n-1}\right) = T^{n-1} \tag{A19}$$

where

$$R^{n-1} = -L^{n-1} + \left[\left(fv\right)^{n-1} - \left(u^2\right)^{n-1}\right]$$

$$T^{n-1} = -M^{n-1} + \left[(fp)^{n-1} - (ug)^{n-1} \right]$$

The corresponding boundary conditions (A7) become

$$\begin{aligned} f_0^n &= 0, \quad u_0^n = 0, \quad g_0^n = 1 \\ u_j^n &= 0, \quad g_j^n = 0 \end{aligned} \tag{A20}$$

If we assume (f_j^{n-1}, u_j^{n-1}, v_j^{n-1}, g_j^{n-1}, p_j^{n-1}), $i = 0, 1, 2, 3, \cdots \cdots$, IMAX with initial values equal to those at the proviso x stations. For higher iterates we get

$$f_j^{(i+1)} = f_j^{(i)} + \delta f_j^{(i)} \tag{A21a}$$

$$u_j^{(i+1)} = u_j^{(i)} + \delta u_j^{(i)} \tag{A21b}$$

$$v_j^{(i+1)} = v_j^{(i)} + \delta v_j^{(i)} \tag{A21c}$$

$$g_j^{(i+1)} = g_j^{(i)} + \delta g_j^{(i)} \tag{A21d}$$

$$p_j^{(i+1)} = p_j^{(i)} + \delta p_j^{(i)} \tag{A21e}$$

We then insert the right side of the expression (A21) in place of f_j^n, u_j^n, v_j^n and g_j^n in Equations (A16)-(A21) dropping the terms that are quadratic in δf_j^i , δu_j^i, δv_j^i and δp_j^i. This procedure yields the following linear system of algebraic equations:

$$f_j^{(i)} + \delta f_j^{(i)} - f_{j-1}^{(i)} - \delta f_{j-1}^{(i)} = \frac{h_j}{2} \left\{ u_j^{(i)} + \delta u_j^{(i)} + u_{j-1}^{(i)} + \delta u_{j-1}^{(i)} \right\}$$

$$\delta f_j^{(i)} - \delta f_{j-1}^{(i)} - \frac{h_j}{2} (\delta u_j^{(i)} + \delta u_{j-1}^{(i)}) = (r_1)_j \tag{A22}$$

$$\delta u_j^{(i)} - \delta u_{j-1}^{(i)} - \frac{h_j}{2} (\delta v_j^{(i)} + \delta v_{j-1}^{(i)}) = (r_4)_j \tag{A23}$$

$$\delta g_j^{(i)} - \delta g_{j-1}^{(i)} - \frac{h_j}{2}\left(\delta g_j^{(i)} + \delta g_{j-1}^{(i)}\right) = (r_5)_j \tag{A24}$$

$$\begin{aligned}&(s_1)_j\,\delta v_j^{(i)} + (s_2)_j\,\delta v_{j-1}^{(i)} + (s_3)_j\,\delta f_j^{(i)} + (s_4)_j\,\delta f_{j-1}^{(i)} + (s_5)_j\,\delta u_j^{(i)} \\ &+ (s_6)_j\,\delta u_{j-1}^{(i)} + (s_7)_j\,\delta g_j^{(i)} + (s_8)_j\,\delta g_{j-1}^{(i)} + (s_9)_j\,\delta p_j^{(i)} + (s_{10})_j\,\delta p_{j-1}^{(i)} = (r_2)_j\end{aligned} \tag{A25}$$

$$\begin{aligned}&(t_1)_j\,\delta p_j^{(i)} + (t_2)_j\,\delta p_{j-1}^{(i)} + (t_3)_j\,\delta f_j^{(i)} + (t_4)_j\,\delta f_{j-1}^{(i)} + (t_5)_j\,\delta u_j^{(i)} \\ &+ (t_6)_j\,\delta u_{j-1}^{(i)} + (t_7)_j\,\delta g_j^{(i)} + (t_8)_j\,\delta g_{j-1}^{(i)} = (r_3)_j\end{aligned} \tag{A26}$$

Where

$$(r_1)_j = f_{j-1}^{(i)} - f_j^{(i)} + h_j u_{j-1/2}^{(i)} \tag{A27a}$$

$$(r_4)_j = u_{j-1}^{(i)} - u_j^{(i)} + h_j v_{j-1/2}^{(i)} \tag{A27b}$$

$$(r_5)_j = g_{j-1}^{(i)} - g_j^{(i)} + h_j p_{j-1/2}^{(i)} \tag{A27c}$$

$$\begin{aligned}(r_2)_j = R_{j-1/2}^{n-1} - &\left\{h_j^{-1}\left(v_j^{(i)} - v_{j-1}^{(i)}\right) + \left(\alpha_1 (fv)'_{j-1/2} + \alpha_2 (u^2)_{j-1/2}^{(i)} - p_3 g'_{j-\frac{1}{2}}\right)\right\} \\ &+ p_4 (pv)'_{j-1/2} - \alpha\left(f_{j-1/2}^{(i)} v_{j-1/2}^{n-1} - f_{j-1/2}^{n-1} v_{j-1/2}^{(i)}\right)\end{aligned} \tag{A27d}$$

$$\begin{aligned}(r_3)_j = T_{j-1/2}^{n-1} - &\frac{1}{P_r} h_j^{-1}\left(p_j^{(i)} - p_{j-1}^{(i)}\right) + \alpha_1 (fp)_{j-1/2}^{(i)} \\ &- \alpha (ug)_{j-1/2}^{(i)} - \alpha\left(u_{j-1/2}^{n-1} g_{j-1/2}^{(i)} - u_{j-1/2}^{(i)} g_{j-1/2}^{n-1} + p_{j-1/2}^{(i)} f_{j-1/2}^{n-1} - p_{j-1/2}^{n-1} f_{j-1/2}^{(i)}\right)\end{aligned} \tag{A27e}$$

Thus the coefficients of momentum equation are

$$(s_1)_j = h_j^{-1} + \frac{\alpha_1}{2} f_j^{(i)} - \frac{\alpha}{2} f_{j-1/2}^{n-1} - \frac{p_4}{2} p_j^{(i)} \tag{A28a}$$

$$(s_2)_j = -h_j^{-1} + \frac{\alpha_1}{2} f_{j-1}^{(i)} - \frac{\alpha}{2} f_{j-1/2}^{n-1} - \frac{p_4}{2} p_{j-1}^{(i)} \tag{A28b}$$

$$(s_3)_j = \frac{\alpha_1}{2} v_j^{(i)} - \frac{\alpha}{2} v_{j-1/2}^{n-1} \tag{A28c}$$

$$(s_3)_j = \frac{\alpha_1}{2} v_j^{(i)} - \frac{\alpha}{2} v_{j-1/2}^{n-1} \tag{A28d}$$

$$(s_5)_j = \alpha_2 u_j^{(i)} \tag{A28e}$$

$$(s_6)_j = -\alpha_2 u_{j-1}^{(i)} \tag{A28f}$$

$$(s_7)_j = P_4 \left[\alpha_1 (fv)_{j-\frac{1}{2}}^{(i)} - \alpha_2 (u^2)_{j-\frac{1}{2}}^{(i)} + \alpha \left(v_{j-\frac{1}{2}}^{i-1} f_{j-\frac{1}{2}}^{i} - v_{j-\frac{1}{2}}^{i} f_{j-\frac{1}{2}}^{i-1} \right) \right] \tag{A28g}$$

$$(s_8)_j = -P_4 \left[\alpha_1 (fv)_{j-\frac{1}{2}}^{(i)} - \alpha_2 (u^2)_{j-\frac{1}{2}}^{(i)} + \alpha \left(v_{j-\frac{1}{2}}^{i-1} f_{j-\frac{1}{2}}^{i} - v_{j-\frac{1}{2}}^{i} f_{j-\frac{1}{2}}^{i-1} \right) \right] \tag{A28h}$$

$$(s_9)_j = -\frac{p_4}{2} v_j^{(i)} \tag{A28i}$$

$$(s_{10})_j = -\frac{p_4}{2} v_{j-1}^{(i)} \tag{A28j}$$

Again the coefficients of energy equation are

$$(t_1)_j = \frac{1}{P_r} h_j^{-1} + \frac{\alpha_1}{2} f_j^{(i)} - \frac{\alpha}{2} f_{j-1/2}^{n-1} \tag{A29a}$$

$$(t_2)_j = -\frac{1}{P_r} h_{j-1}^{n-1} + \frac{\alpha_1}{2} f_{j-1}^{(i)} - \frac{\alpha}{2} f_{j-1/2}^{n-1} \tag{A29b}$$

$$(t_3)_j = \frac{\alpha_1}{2} p_j^{(i)} + \frac{\alpha}{2} p_{j-1/2}^{n-1} \tag{A29c}$$

$$(t_4)_j = \frac{\alpha_1}{2} p_{j-1}^{(i)} + \frac{\alpha}{2} p_{j-1/2}^{n-1} \tag{A29d}$$

$$(t_5)_j = -\frac{\alpha}{2} g_j^{(i)} + \frac{\alpha}{2} g_{j-1/2}^{n-1} \tag{A29e}$$

$$(t_6)_j = -\frac{\alpha}{2} g_{j-1}^{(i)} + \frac{\alpha}{2} g_{j-1/2}^{n-1} \tag{A29f}$$

$$(t_7)_j = -\frac{\alpha}{2} u_j^{(i)} - \frac{\alpha}{2} u_{j-1/2}^{n-1} \tag{A29g}$$

$$(t_8)_j = -\frac{\alpha}{2} u_{j-1}^{(i)} - \frac{\alpha}{2} u_{j-1/2}^{n-1} \tag{A29h}$$

$$(t_9)_j = 0 \tag{A29i}$$

$$(t_{10})_j = 0 \tag{A29j}$$

The boundary condition (A7) becomes

$$\partial f_0 = 0\,,\ \partial u_0 = 0\,,\ \partial \theta_0 = 1$$

$$\partial u_j = 0,\ \partial \theta_j = 0 \tag{A30}$$

which just express the requirement for the boundary conditions to remain during the iteration process. Now the system of linear Equations (A27) and (A28) together with the boundary

conditions (A29) can be written in matrix or vector form, where the coefficient matrix has a block tri-diagonal structure. The whole procedure, namely reduction to first order followed by central difference approximations. Newton's quasi-linearization method and the block Thomas algorithm, is well known as the Keller- box method.

References

Ahmad, N. and Zaidi, H. N., 'Magnetic effect on oberback convection through vertical stratum'. *2nd BSME-ASME International Conference on Thermal Engineering*, Vol.1,pp. 157-168, (2004).

Cebeci T.and Bradshaw P., Physical and Computational Aspects of Convective Heat Transfer, Springer, New York (1984)

Cheng. P., 'Mixed convection about a horizontal cylinder and a sphere in a fluid –saturated porous medium'. *Int. J Heat Mass Transfer.*, Vol.25,No.1, pp. 1245-1247, (1982).

Chowdhury, M.K. and Islam, M.N., 'MHD free convection flow of visco-elastic fluid past an infinite porous plate', *Heat and Mass Transfer*, Vol.36, pp. 439-447. (2000).

Clarke J.F. and Riley N., 'Natural convection induced in a gas by the presence of a hot porous horizontal surface', *Q. J. Mech. Appl. Math.*, Vol. 28, pp. 373–396, (1975).

Clarke J.F. and Riley N., 'Free convection and the burning of a horizontal fuel surface', J. Fluid Mech., Vol.74, pp. 415–431. (1976).

Cogley A.C., Vincenti W.G. and Giles S.E., 'Differential approximation for radiation transfer in a nongray near equilibrium', *AIAA Journal* . Vol.6 , pp. 551–553, (1968).

Elbashbeshy, E. M. A., 'Free convection flow with variable viscosity and thermal diffusivity along a vertical plate in the presence of magnetic field', *Int. J. Engineering Science*, Vol. 38, pp. 207-213, (2000).

Hossain, M.A. and Ahmad, M. , 'MHD forced and free convection boundary layer flow near the leading edge', *Int. J. Heat Mass Transfer*, Vol.33, No. 3, pp. 571-575, (1990).

Hossain. M .A., 'Viscous and joule heating effects on MHD-free convection flow with variable plate temperature', *Int. J Heat Mass Transfer.*, Vol.35, No.12, pp. 3485-3487, (1992).

Hossain M. A. and Takhar H. S, 'Radiation effect on mixed convection along a vertical plate with uniform surface temperature', *Heat and Mass Transfer*, Vol. 31, pp. 243-248, (1996).

Hossain, M.A., Alam, K.C.A. and Rees, D.A.S., 'MHD forced and free convection boundary layer flow along a vertical porous plate', *Applied Mechanics and Engineering*, Vol.2, No. 1, pp. 33-51, (1997).

Hossain, M. A. and Alim, M. A., Natural convection-radiation interaction on boundary layer flow along a Thin cylinder, *J. Heat and Mass Transfer*, Vol. 32, pp. 515-520, (1997).

Hossain, M .A., Das, S. K. and Pop, I., 'Heat transfer response of MHD free convection flow along a vertical plate to surface temperature oscillation', *Int.J. Non- Linea Mechanics*, Vol. 33, No. 3, pp. 41-553, (1998).

Huang, M.J. and Chen, C.K., 'Laminar free convection from a sphere with blowing and suction', *J. Heat Transfer*, Vol. 109, pp. 529-532, (1987).

Keller H.B., 'Numerical methods in boundary layer theory, Annual Rev. Fluid Mechanics', Vol. 10. pp. 417-433, (1978).

Keller, H. B. and Cebeci, T, 'Accurate numerical methods for boundary layer flows, part-I. Two–dimensional laminar flows', Proceedings of the Second International Conference on numerical Methods in fluid dynamics, Springer, New York, p. 92, (1971).

Kimura, S. ,Okajima, A. and Kiwata, T. 'Conjugate natural convection from a vertical heated slab'. *Int. J. Heat and Mass Transfer*, Vol. 41, pp. 3203-3211, (1998).

Kuiken. H. K., 'Magneto-hydrodynamic free convection in strong cross flow field', *J. Fluid Mech.*, Vol. 40, pp. 21-38, (1970).

Lin H.T. and Yu W.S., 'Free convection on a horizontal plate with blowing and suction, J. Hear Trans.', *Trans. ASME* , Vol. 110, pp. 793–796, (1988).

Mendez, F. and Trevino, C., 'The conjugate conduction-natural convection heat transfer along a thin vertical plate with non-uniform internal heat generation', *Int. J. Heat and Mass Transfer*, Vol. 43, pp. 2739-2748, (2000).

Merkin, J.H. and Mahmood, T., 'On the free convection boundary layer on a vertical plate with prescribed surface heat flux', *J. Engg. Math*, Vol. 24, pp. 95-107, (1990).

Merkin,J.H. and Pop,I. 'Conjugate free convection on a vertical surface'. *Int. J Heat Mass Transfer*, Vol. 39, pp. 7, 1527-1534, (1982).

Miyamoto, M., Sumikawa, J., Akiyoshi , T. and Nakamura,T., 'Effects of axial heat conduction in a vertical flat plate on free convection heat transfer', *Int. J Heat Mass Transfer*, Vol. 23, pp. 1545-1553, (1980).

Molla, M.M., Hossain, M.A. and Yao, L.S., 'Natural convection flow along a vertical wavy surface with uniform surface temperature in presence of heat generation / absorption', *Int. J. Thermal Science*, Vol. 43, pp. 157-163, (2004).

Molla, Md. M., Taher, M.A., Chowdhury, Md. M. K. and Hossain. Md. A. Magnetohydrodynamic Natural Convection Flow on a Sphere in Presence of Heat Generation, *J. Nonlinear Analysis: Modelling and Control*, Vol. 10, No. 4, pp. 349-363, (2005).

Nazar, R., Amin, N. and Pop, I., 'Free convection boundary layer flow on a horizontal circular cylinder with constant heat flux in a micropolar fluid', *Int. Comm. Heat Mass Transfer*, Vol. 7, No. 2, pp. 409-431, (2002a).

Nazar, R., Amin, N., Grosan, T. and Pop, I., 'Free convection boundary layer on an isothermal sphere in a micropolar fluid', *Int. Comm. Heat Mass Transfer*, Vo. 29, No.3, pp. 377-386, (2002b).

Özisik M. N., Radiative Transfer and Interactions with Conduction and Convection, Wiley, New York, (1973).

Pozzi,A. and Lupo,M. 'The coupling of conduction with laminar natural convection along a flat plate', *Int. J Heat Mass Transfer*, Vol. 31, No.8, pp. 1807-1814, (1988).

Raptis, A. and Kafousian, N. (1982), 'Magnetohydrodynamic free convection flow and mass transfer through a porous medium bounded by an infinite vertical porous plate with constant heat flux', *Canadian Journal of Physics*, Vol. 60, No.12, pp. 1725-1729, (1982).

Soundalgekar V.M., Takhar H.S. and Vighnesam N.V., 'The combined free and forced convection flow past a semi-infinite vertical plate with variable surface temperature', *Nuclear Engineering and Design* , Vol.110, pp. 95-98, (1960).

Sparrow, E. M. and Cess, R. D., 'Effect of magnetic field on free convection heat transfer'.*Int. J. Heat mass Transfer*, Vol. 3, pp. 267. (1961).

Taher, M. A., Chowdhury, M. M. K. and Molla, M.M., 'Magnetohydrodynamic natural convection flow on a sphere', *proceeding of the 4th International conference on Mechanical Engineering and 9th annual paper meet*, Dhaka, pp. 85-91, (2004).

Taher, M. A. and Molla, M. M., 'Natural convection boundary layer flow on a sphere in presence of heat generation', *proceeding of the 5th International conference on Mechanical Engineering and 10th annual paper meet*, Dhaka, pp. 223-228, (2005).

Vajravelu, K. and Hadjinicolaou, A., 'Heat transfer in a viscous fluid over a stretching sheet with viscons dissipation and internal heat generation', *Int. Comm. Heat Mass Transfer*, Vol. 20, pp. 417-430, (1993).

Vedhanayagam M., Altenkirch R. A. and Eichhorn R. , 'A transformation of the boundary layer equations for free convection past a vertical flat plate with arbitrary blowing and wall temperature variations', *Int. J. Heat Mass Tran.*, Vol. 23, pp. 1286-1288, (1980).

Vynnycky, M. and Kimura,S. 'Conjugate free convection due to heated vertical plate', *Int. J Heat Mass Transfer.*, Vol. 38, No. 5, pp. 1067-1080, (1982).

Yao, L.S., 'Natural convection along a vertical wavy surface'. *ASME J. Heat Transfer*, Vol. 105, pp. 465-468, (1983).

Yu, W-S. and Lin, H-T., 'Conjugate Problems of conduction and free convection on vertical and horizontal flate plate', *Int. J Heat Mass Transfer.*, Vol. 36, No.5, pp. 1303-1313, (1982).